Pergamon

Journal of Structural Geology, Vol. 19, No. 2, pp. 139 to 157, 1997

PII: S0191-8141(96)00084-3
0191-8141/97 $17.00 + 0.00

Progressive deformation of the Chugach accretionary complex, Alaska, during a paleogene ridge–trench encounter

TIMOTHY M. KUSKY

Department of Earth Sciences, Boston University 675, Commonwealth Ave., Boston, MA 02215, U.S.A.

DWIGHT C. BRADLEY and PETER HAEUSSLER

United States Geologic Survey, Branch of Alaskan Geology, 4200 University Drive, Anchorage, AK 99508, U.S.A.

(*Received* 29 *November* 1995; *accepted in revised form* 26 *September* 1996)

Abstract—The Mesozoic accretionary wedge of south-central Alaska is cut by an array of faults including dextral and sinistral strike-slip faults, synthetic and antithetic thrust faults, and synthetic and antithetic normal faults. The three fault sets are characterized by quartz ± calcite ± chlorite ± prehnite slickensides, and are all relatively late, i.e. all truncate ductile fabrics of the host rocks. Cross-cutting relationships suggest that the thrust fault sets predate the late normal and strike-slip fault sets. Together, the normal and strike-slip fault system exhibits orthorhombic symmetry. Thrust faulting shortened the wedge subhorizontally perpendicular to strike, and then normal and strike-slip faulting extended the wedge oblique to orogenic strike. Strongly curved slickenlines on some faults of each set reveal that displacement directions changed over time. On dip-slip faults (thrust and normal), slickenlines tend to become steeper with younger increments of slip, whereas on strike-slip faults, slickenlines become shallower with younger strain increments. These patterns may result from progressive exhumation of the accretionary wedge while the faults were active, with the curvature of the slickenlines tracking the change from a non-Andersonian stress field at depth to a more Andersonian system (σ_1 or σ_2 nearly vertical) at shallower crustal levels.

We interpret this complex fault array as a progressive deformation that is one response to Paleocene–Eocene subduction of the Kula–Farallon spreading center beneath the accretionary complex because: (1) on the Kenai Peninsula, ENE-striking dextral faults of this array exhibit mutually cross-cutting relationships with Paleocene–Eocene dikes related to ridge subduction; and (2) mineralized strike-slip and normal faults of the orthorhombic system have yielded $^{40}Ar/^{39}Ar$ ages identical to near-trench intrusives related to ridge subduction. Both features are diachronous along-strike, having formed at circa 65 Ma in the west and 50 Ma in the east. Exhumation of deeper levels of the southern Alaska accretionary wedge and formation of this late fault array is interpreted as a critical taper adjustment to subduction of progressively younger oceanic lithosphere yielding a shallower basal décollement dip as the Kula–Farallon ridge approached the accretionary prism. The late structures also record different kinematic regimes associated with subduction of different oceanic plates, before and after ridge subduction. Prior to triple junction passage, subduction of the Farallon plate occurred at nearly right angles to the trench axis, whereas after triple junction migration, subduction of the Kula plate involved a significant component of dextral transpression and northward translation of the Chugach terrane. The changes in kinematics are apparent in the sequence of late structures from: (1) thrusting; (2) near-trench plutonism associated with normal + strike-slip faulting; (3) very late gouge-filled dextral faults.

GEOLOGIC SETTING

Alaska's Pacific margin is underlain by two parallel composite terranes or 'superterranes' — the Wrangellia superterrane (consisting of the Peninsular, Wrangellia, and Alexander Terrane), and farther outboard, the Chugach–Prince William superterrane (Fig. 1a & b) (Nokleberg *et al.*, 1989, 1994; Plafker *et al.*, 1994). During much of the Mesozoic, the two superterranes formed a magmatic arc and accretionary wedge, respectively, above a circum-northeast Pacific subduction zone (Nokleberg *et al.*, 1989, 1994; Plafker *et al.*, 1994; Plafker and Berg, 1994). The Mesozoic part of the accretionary wedge (Chugach terrane) has been broken out from the slightly younger Cenozoic part (Prince William terrane). The faults analyzed for this project cut the Chugach terrane, which consists of accreted ocean floor rocks that range from fairly coherent to thoroughly disrupted mélange. In south-central Alaska (Fig. 2), the Chugach terrane contains two major units. Farther inboard lies the McHugh Complex, composed mainly of basalt, chert, argillite, and graywacke (Clark, 1973; Bradley and Kusky, 1992). Radiolaria from McHugh Complex cherts throughout south-central Alaska range in age from Ladinian (middle Triassic) to Albian–Aptian (mid-Cretaceous) (Nelson *et al.*, 1987; C. Blome, written communication, 1994). The interval during which the McHugh Complex formed by subduction–accretion is not well known, but probably spanned most of the Jurassic and into the middle Cretaceous. The McHugh has been thrust seaward on the Eagle River fault over a relatively coherent tract of trench turbidites (Nilsen and Zuffa, 1982) of the Upper Cretaceous Valdez Group (Fig. 2).

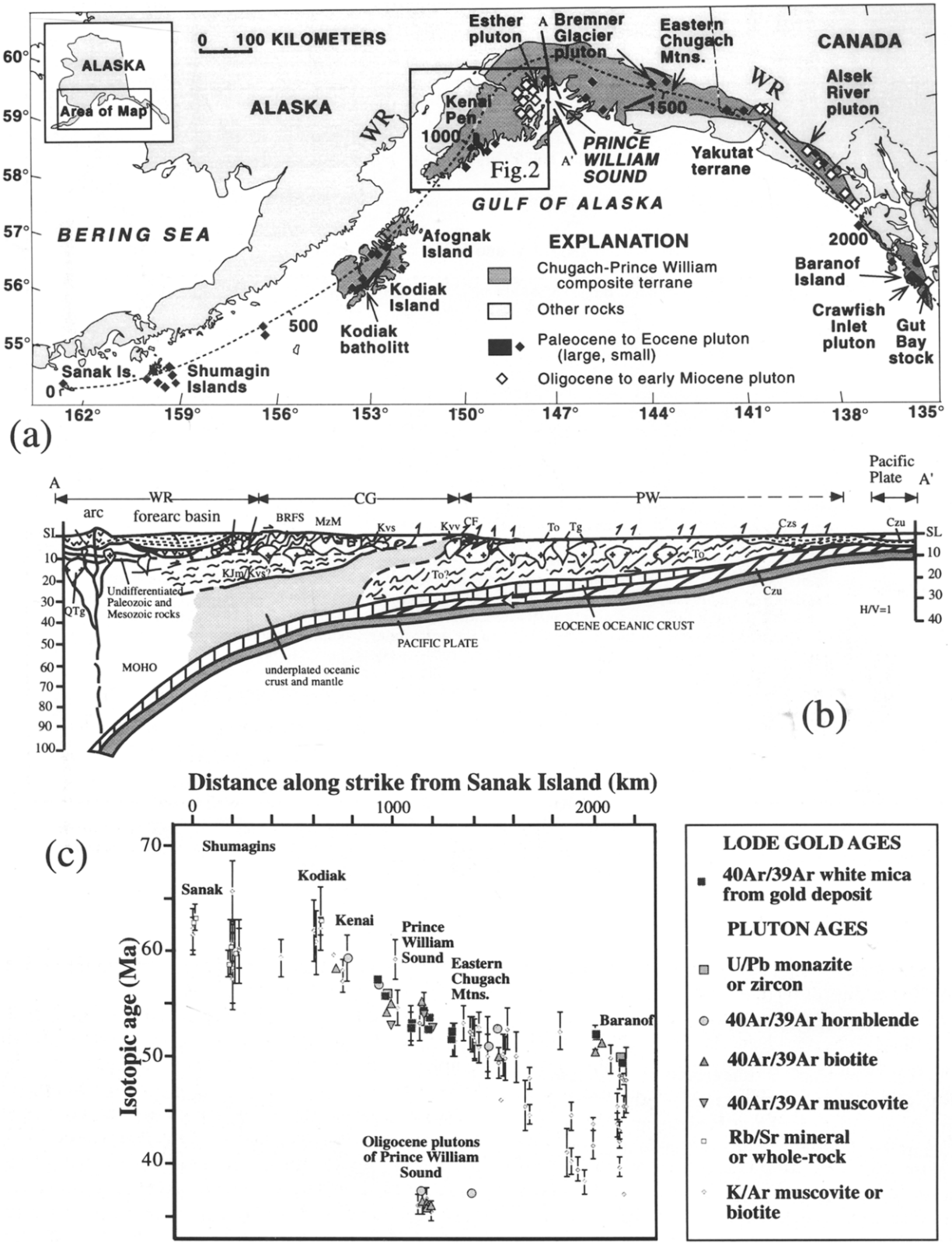

Fig. 1. Generalized map (a) and cross-section (b) of south-central Alaska showing Chugach–Prince William composite terrane situated south of the Wrangellia composite terrane (map after Bradley *et al.*, 1994; cross-section after Plafker *et al.*, 1994). Box shows locations of Fig. 2. Abbreviations as follows; WR = Wrangellia, CG = Chugach terrane, PW = Prince William terrane, MzM = McHugh Complex, BRFS = Border Ranges fault system, Kvs = Valdez Group sedimentary rocks, Kvv = Valdez Group volcanic rocks, To = Paleocene and Eocene Orca Group, Tg = Tertiary granitic rocks, Czs = Cenozoic marine sedimentary rocks, Czu = Late Cenozoic deep marine sedimentary rocks, Qtg = Quaternary and Tertiary intrusive rocks. (c) Age vs distance along strike plot of Sanak–Baranof magmatic belt showing age progression of plutonism, and age of lode gold deposits, which show a similar age progression. Modified after Bradley *et al.* (1993) and Haeussler *et al.* (1995).

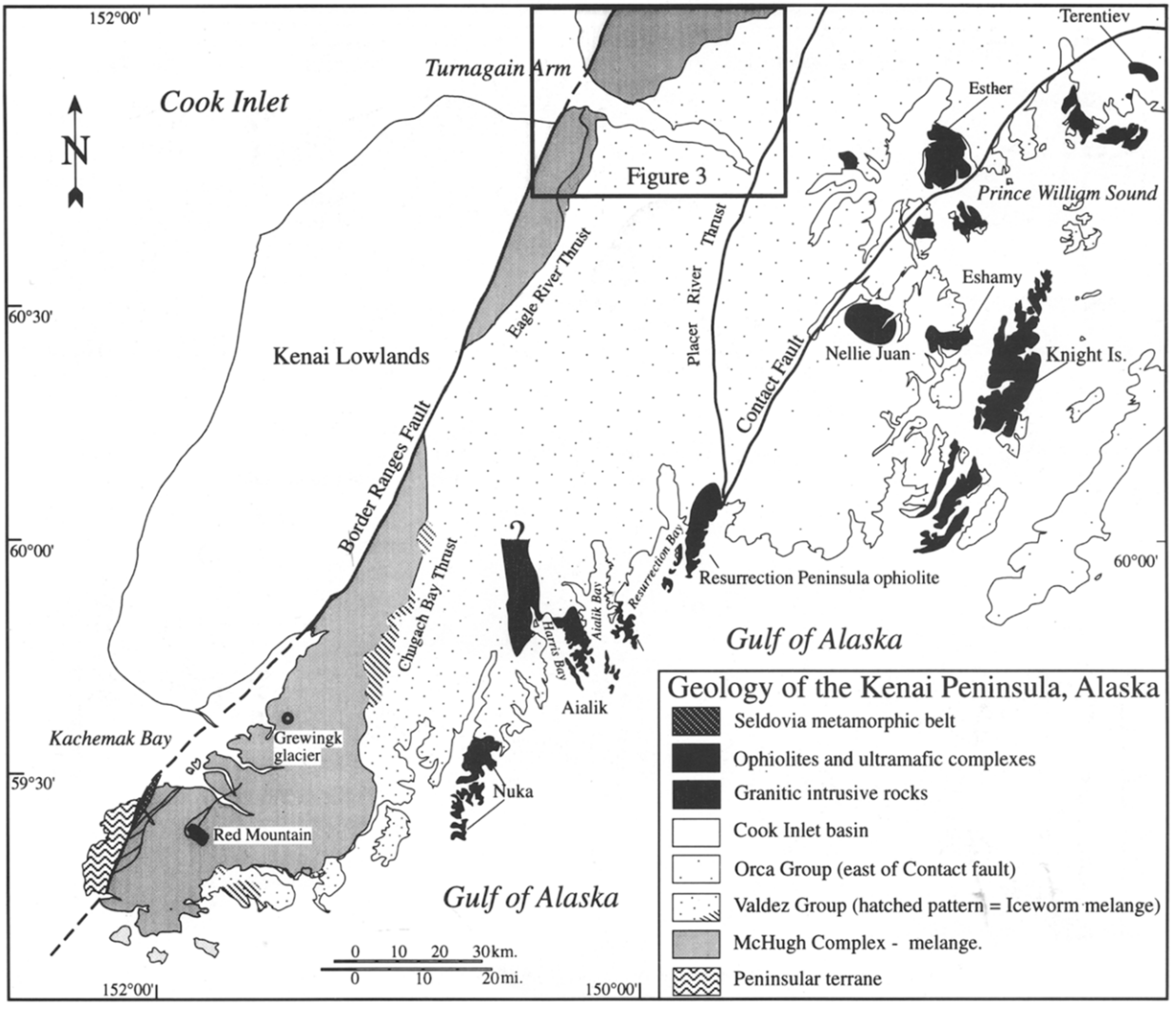

Fig. 2. Simplified bedrock geologic map of the Kenai Peninsula, showing setting of Turnagain Arm study area, and other locations described in text. Border Ranges fault separates Peninsular (Wrangellian superterrane) and Chugach terranes, and Contact fault separates Chugach and Prince William terranes.

After the protracted episode of subduction–accretion that built the Chugach terrane, the accretionary wedge was intruded by near-trench intrusive rocks of the Sanak–Baranof plutonic belt (Hudson, 1979, 1983), which several authors have related to subduction of the Kula–Farallon spreading center (Marshak and Karig, 1977; Hill *et al.*, 1981; Sisson *et al.*, 1989; Bradley *et al.*, 1993; Pavlis and Sisson, 1995). The near-trench magmatic pulse migrated 2200 km along the continental margin, from about 63–65 Ma in the west to about 50 Ma in the east (Bradley *et al.*, 1993). In the Turnagain Arm area, the magmatism occurred at about 55–52 Ma (Fig. 1c). Evidence that Paleogene near-trench magmatism was related to subduction of the Kula–Farallon spreading center, reviewed by Bradley *et al.* (1993), consists of: (1) the diachronous nature of the magmatism; (2) near-trench position of the magmatism, in a location normally cold and under compression; and (3) geochemical evidence that the magmas represent a mixture of MORB sources and partially melted accretionary prism material (see also Harris *et al.*, 1996).

The study area along Turnagain Arm (Figs 2 & 3) includes rocks of the Valdez Group and McHugh Complex. The northwestern, inboard part of the McHugh Complex's outcrop belt is a mélange composed of fragments and disrupted beds of greenstone, chert, and graywacke in a deformed matrix of argillite (Clark, 1973; Bradley and Kusky, 1990). The southeastern part of the outcrop belt is mainly composed of siliciclastic rocks, including boulder and cobble conglomerate, graywacke, and argillite; bedding is laterally discontinuous in the rare places where it can be observed. Throughout the McHugh Complex, moderate to intense stratal disruption has resulted in tectonic juxtaposition of varied rock types, at all scales (Bradley and Kusky, 1992). Clark (1973) reported prehnite–pumpellyite metamorphic facies assemblages in the McHugh Complex in the study area. The mélange foliation, early ductile shear zones,

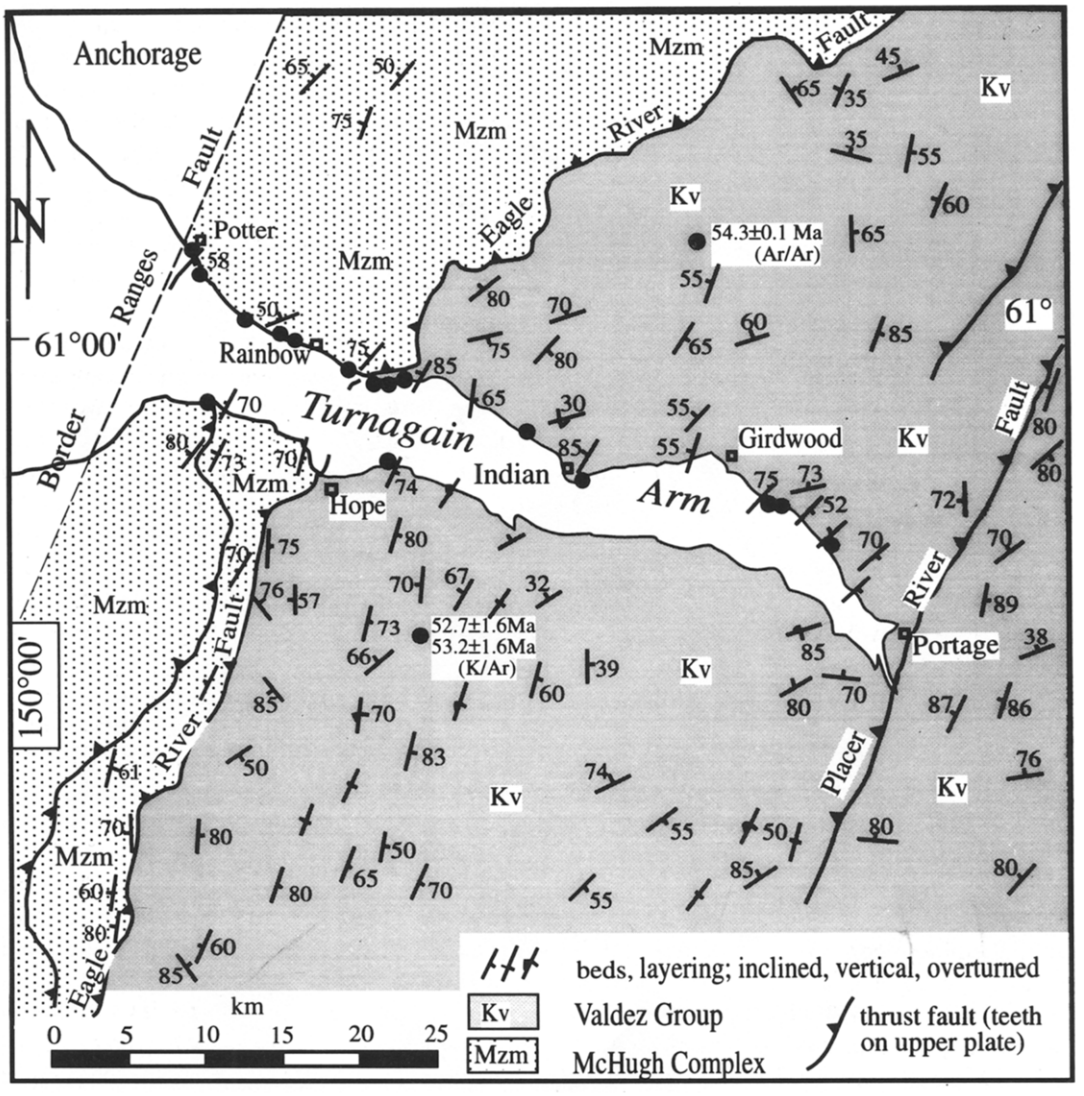

Fig. 3. Geologic map of Turnagain Arm. Dots indicate locations where minor faults were studied. Ten localities are in the McHugh Complex; nine are in the Valdez Group. Mzm, Mesozoic McHugh Complex; Kv, Cretaceous Valdez Group. Faults dashed where concealed. Also shown are ages of syn-faulting veins. Modified from Magoon *et al.* (1976).

and contorted prehnite veinlets are cut by abundant brittle faults that contribute to the chaotic appearance of these rocks.

The Upper Cretaceous Valdez Group (Fig. 3) consists of turbidites composed of graywacke, siltstone, black argillite, and minor pebble to cobble conglomerate (Dumoulin, 1987). Graded beds in the Valdez Group exhibit a refracted slaty cleavage that is strong in argillite and weak in graywacke. Brittle faults like those in the McHugh Complex cut bedding and cleavage in the Valdez Group (Bradley and Kusky, 1990).

The Eagle River fault along Turnagain Arm is marked by a 1–1.5 km wide Type I mélange (*sensu* Cowan, 1985), that is correlative with: (1) the Iceworm mélange of the southern Kenai Peninsula (Kusky *et al.*, 1993); and (2) the mélange of Waterfall Bay on Afognak Island (Fisher and Byrne, 1987). The mélange formed during thrusting of the already metamorphosed McHugh Complex over the Valdez Group (underplating of the Valdez Group), causing intense stratal disruption via layer parallel extension.

Along Turnagain Arm, a late fault array consisting of three sets of late faults is present: (1) NNE-striking and ENE-striking thrust faults, (2) a conjugate pair of NE-striking dextral and NW-striking sinistral-slip faults, and (3) a conjugate set of WNW-striking normal faults. Together the strike-slip and normal faults possess orthorhombic symmetry, whereas the orientation of the thrusts is misoriented by 45° from the symmetry plane, giving the entire fault array monoclinic symmetry. This study presents a detailed kinematic analysis of these late faults (Bradley and Kusky, 1990). In addition, the study: (1) assesses slip lineations on this fault array in terms of the simplest strain history that can explain the complex patterns and still be consistent with the regional structural evolution; and (2) discusses implications of

our findings for the tectonic history of this accretionary wedge.

MACROSCOPIC DESCRIPTION OF BRITTLE FAULTS

Minor faults were examined along a 43 km transect across the strike of the accretionary complex in Turnagain Arm (Figs 2 & 3). The faults are abundantly exposed in highway and railroad cuts, and in weathered coastal exposures on both sides of Turnagain Arm (Bradley and Kusky, 1990). The faults juxtapose rock types assigned to a single map unit (McHugh Complex or Valdez Group) and account for some of the discontinuity of rock types that has frustrated attempts at subdivision of these two major units along Turnagain Ann (Clark, 1973, pp. D5–D9). Attitudes of 140 faults with associated slickenline orientations and stepping directions were measured at locations shown in Fig. 3. The data set includes only faults from which unambiguous kinematic information could be obtained using stepping directions on slickenside surfaces. We discerned no systematic difference in orientation of fault planes and lineations between the McHugh Complex and Valdez Group, consistent with the conclusion that the two were juxtaposed prior to formation of the late faults (Kusky *et al.*, 1993). Thus we present the data from both units together here.

Prominent slickenfibers composed of quartz, calcite, chlorite, or rarely prehnite mark slickenside surfaces; slickenlines (*sensu* Fleuty, 1974) with fiber-steps clearly reveal shear sense (Fig. 4). Bands of wall-rock fragments and a lack of medial sutures reveals that fiber growth was antithetic (Fig. 4). The youngest increments of growth are therefore adjacent to fiber steps, and the oldest increments are in the center of individual fibers. Faults are categorized as reverse or normal for slickenline rakes greater than 45°, or dextral or sinistral for rakes less than 45°. Where appropriate, faults with two superimposed sets of slickenlines or a single set of curved slickenlines are assigned to two groups. Mean directions of lineations or poles quoted below are calculated from equal area scatter plots (Fig. 5) superimposed on contour diagrams. The stereoplots reveal three main sets of faults on the basis of attitude and slip direction, which are summarized in Fig. 6(a–c).

All three fault sets include examples with straight and curved fibrous slickenlines that consist of quartz, calcite and chlorite. Owing to lack of markers, the magnitude of displacement is rarely evident, but locally observable offsets range from a few tens of centimeters to a few meters. Most faults are a few meters to greater than 20 m in length. The fault zones are typically less than 5 cm thick, consistent with the observed displacements. They were responsible for significant regional deformation because, although individual displacements are small, the faults are spaced every few meters to tens of meters. Similar slickenfiber geometry, mineralogy, and sequence of mineral growth suggest that the three main fault sets — thrust (synthetic and antithetic), conjugate strike-slip, and normal (synthetic and antithetic) faults formed under similar deformational conditions. However, a limited number of cross-cutting relationships suggest that the thrust faults are slightly older than the other strike-slip and normal faults. Several young steep dextral/oblique thrusts marked by unmetamorphosed gouge zones a few cm thick cross all other faults and appear to be the youngest structures present, and are not included in the late fault array discussed here. Other cross-cutting relationships include two sinistral faults cutting older thrusts, a normal fault cutting an older thrust, a dextral strike-slip fault cutting a dip-slip fault (260, 46°N, lineation pitch 79°W), a dextral fault cutting a thrust, and a thrust cutting an older thrust. No late thrusts were observed cutting other late faults. These cross-cutting relationships are supported by numerous other observations of late normal, dextral and sinistral strike-slip faults, and near-trench dikes, cutting each other on the southern Kenai Peninsula (Kusky, Bradley, and Haeussleur, unpub. field notes; Haeussler and Bradley, 1996), and elsewhere in southern Alaska, as described below.

Thirty one of the faults in the data set are reverse faults. Following Butler (1982), the term 'thrust' is used for all reverse faults, regardless of dip angle. Most of the thrusts (21) are synthetic (landward-dipping) thrusts with SSW strikes (mean strike is 207°), and NW dips (mean 62°) (Fig. 5a & b). One third (10) are antithetic thrusts that strike east-northeast (078°) and dip southeast (54°). The mean hangingwall movement direction of synthetic thrusts is 102° up-dip, whereas the hangingwall for the antithetic thrusts moved towards 311°. The mean attitude of synthetic thrusts is subparallel to the mélange foliation in the McHugh Complex and bedding in the Valdez Group, and the mean slip lineation for the thrust faults is not perpendicular to the fault intersection, suggesting that the thrusts may have reactivated older anisotropies such as bedding and early foliations related to accretion/offscraping in mélange of the McHugh Complex and turbidites of the Valdez Group. Nonetheless, the orientation of these faults suggests roughly NW–SE contraction and compression, roughly perpendicular to orogenic strike. Thrusts are present throughout the study area, but they are abundant only directly east of, and structurally below, the two map-scale faults: (1) a regional thrust fault (a segment of the Border Ranges fault known as the Knik fault) exposed at the Potter Marsh weigh station (Fig. 3), which cuts mélange of the McHugh Complex, and (2) a fault exposed near Indian, 5 km east of Rainbow (Fig. 3), which cuts metasedimentary rocks of the Valdez Group in the Iceworm mélange forming the strongly deformed footwall of the Eagle River fault. Assuming that the outcrop-scale structures reflect the regional map-scale structures (Wojtal, 1989), the concentration of minor thrusts in these two areas

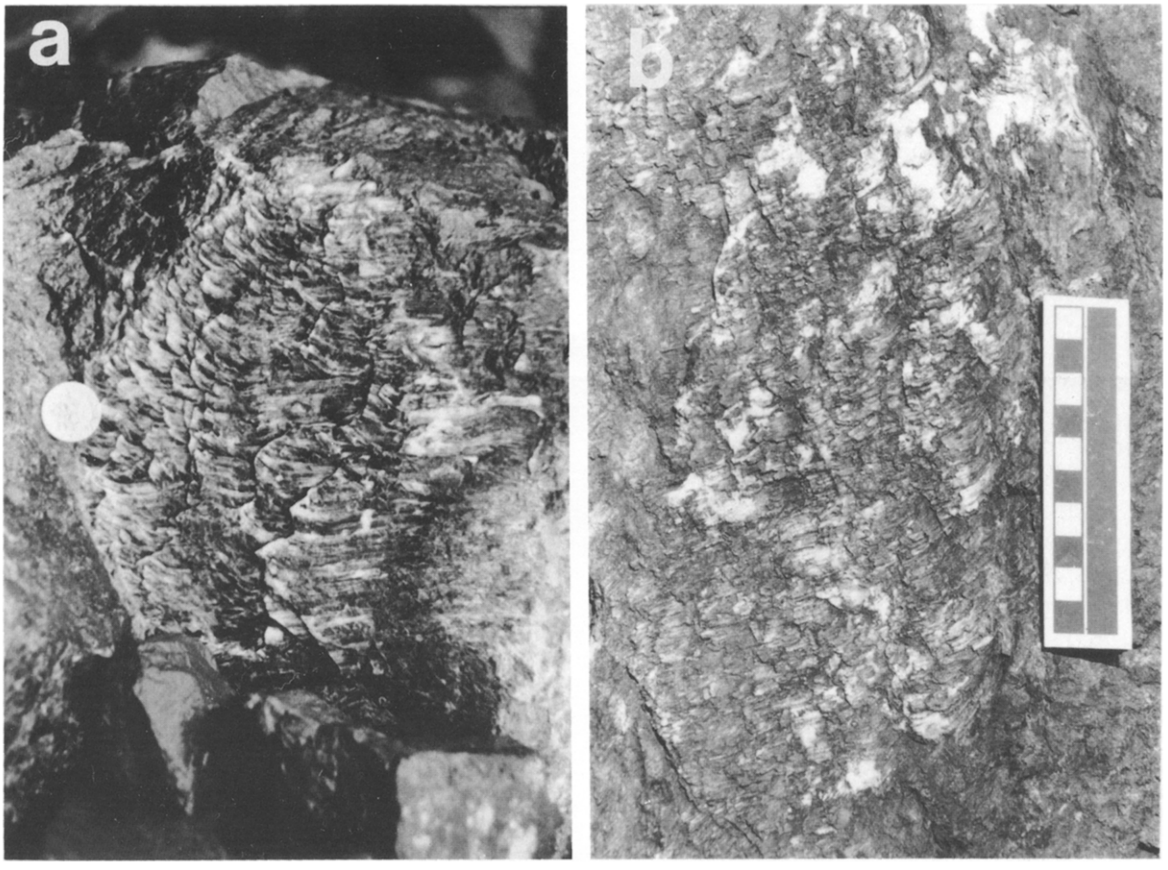

Fig. 4. High-angle fault surfaces with curved fibrous slickenlines. Fibers are antitaxial, with youngest part of a given slickenline immediately adjacent to step where it ends, as shown by common wall rock inclusions (dark bands) and lack of medial sutures.

suggests that both major faults are thrusts (Magoon *et al.*, 1976; Bradley and Kusky, 1990; Winkler, 1992; Kusky *et al.*, 1993).

The data set also includes 18 normal faults. Despite some scatter (Fig. 5d), most of which strike east-southeast (mean 100°) and dip southwest (mean 46°). The mean hangingwall movement direction is about 210°. One normal fault has an antithetic attitude (270°, 37°N) relative to this major set (Figs 5 & 6), and records a hangingwall movement direction towards 321°.

Abundant dextral faults (61 examples) strike east-northeast (mean 053°) and dip steeply south (mean 71°); the sinistral faults (30 examples), strike southeast (mean 141°), and dip steeply southwest (mean 81°). Strike-slip faults of both sets are ubiquitous throughout the study area in both the McHugh Complex and Valdez Group.

Sets of dextral and sinistral strike-slip faults (Fig. 5e & g) form what in Andersonian terms would be interpreted as a conjugate pair, consistent with their mean slip lineations being perpendicular to the fault intersections. The slip lineations for the normal faults are also nearly perpendicular to the fault intersection, consistent with their being a conjugate set as well. However, the strike-slip and normal faults appear roughly contemporaneous, and have the same symmetry axis. We suggest that together they represent an orthorhombic fault system, reflecting a general three-dimensional non-plane strain (Reches, 1983; Krantz, 1989). Figure 6(d) shows our interpretation of these faults as an orthorhombic set, suggesting roughly E–W contraction, N–S (orogen-oblique) extension, plus a component of vertical shortening. This reflects a significant change from the NW–SE contraction inferred from the attitude of the older thrust faults.

CURVED SLICKENLINES

Many of the brittle faults along Turnagain Arm have slickenlines that are curved by as much as 55° within the fault plane (Fig. 4). Figure 7(a & b) reveals that faults with straight slickenlines have a 360° range in strikes whereas faults with curved slickenlines have only a 180° range (between 050° and 230°; strike directions assigned according to the right-hand rule). The significance of this finding is unclear, but may be related to unfavorable slip plane orientations in a progressively changing structural setting. Stepping directions provide a basis for determining the sense of offset on individual faults; hence faults may be classified as either clockwise (22 examples) or

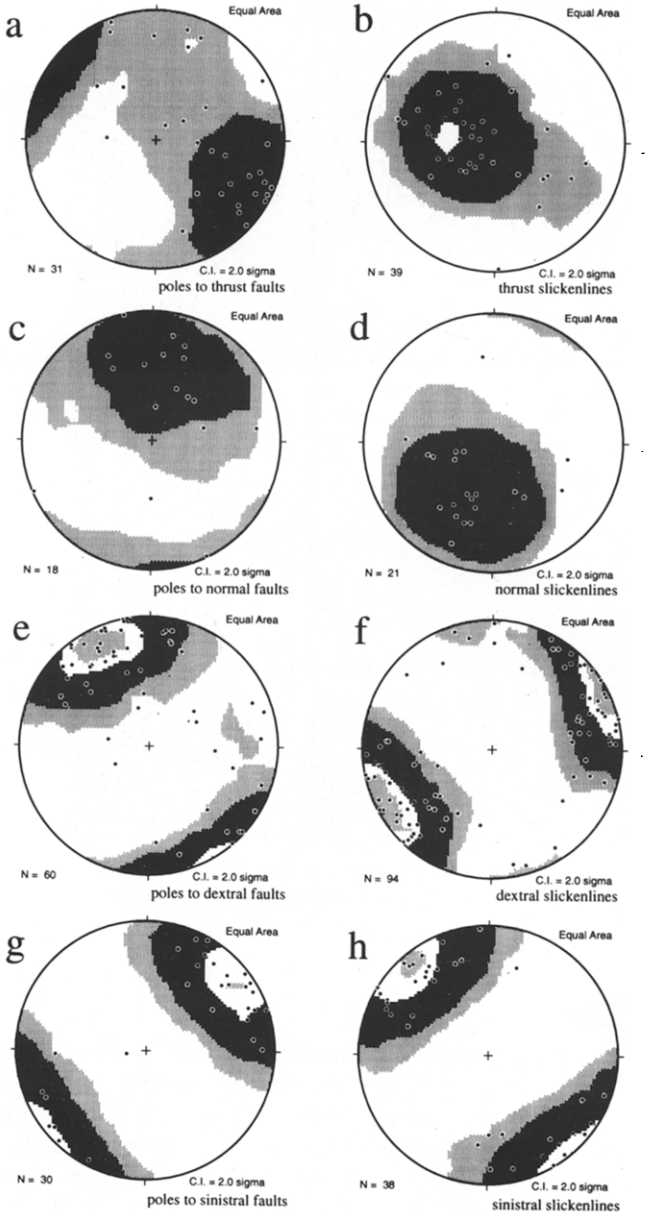

Fig. 5. Lower hemisphere equal area projections for fault plane and slickenlines from localities shown in Fig. 2. Slickenline data include orientation of straight fibers, as well as the beginning and ending orientations of curved fibers. (a) Poles to thrust-fault planes (synthetic thrust faults dip to the northwest, whereas antithetic thrust faults dip southwest). (b) Thrust-fault slickenlines. (c) Poles to normal-fault planes. (d) Normal-fault slickenlines. (e) Poles to dextral-fault planes. (f) Dextral-fault slickenlines. (g) Poles to sinistral-fault planes. (h) Sinistral slickenlines.

counterclockwise (29 examples) on the basis of the sense of slickenline curvature when the fault plane was viewed from above along an outward pointing normal (Fig. 8). To assess the significance and origin of the curvature of the curved slickenlines, the data are here analyzed using equal area projections, slip-direction trajectories, and tangent lineation diagrams; analysis using kinematic rotation axes (Twiss and Gefell, 1990) was found to be ambiguous.

Slip-direction trajectories

Slip-direction trajectories are constructed by plotting the beginning and ending orientations of individual curved slickenfibers. These may be plotted because the fibers grew antitaxially, as shown by the common wall-rock fragments and lack of medial sutures. Counter-clockwise slickenlines converge toward a SW-plunging zone (Fig. 8a), whereas clockwise slickenlines diverge from a SW-dipping girdle (Fig. 8b). On several strike-slip faults, slickenline curvature was sufficient to change the plunge direction of the instantaneous slip vector. Where this occurred on non-vertical faults, the component of dip-slip motion must have changed sense as the plunge direction of the slickenlines changed. Thus, judging from present attitudes, several faults in Turnagain Arm appear to have evolved from transpressional to transtensional structures (and vice versa) during fault motion.

Additional insight to the kinematics of these faults is gained by plotting thrust, normal, and strike-slip faults separately. Figure 9(a) shows that curved slickenfibers on thrust faults possess a counter-clockwise spin converging on a steeply southwesterly plunging zone. Curved slickenfibers on normal faults similarly converge on a southwesterly plunging zone (Fig. 9b). Curved slickenfibers on strike-slip faults show convergence towards shallowly NW- and SW-plunging zones for sinistral and dextral faults, respectively (Fig. 9c & d). These patterns reveal that slip lineations on dip-slip faults tend towards steeper attitudes with younger slip increments, whereas slip lineations on strike-slip faults tend towards shallower orientations with time. The zones of convergence (eyeball best-fit) for each set of lineations corresponds to the mean slip lineation for each data set (compare Figs 9 & 6).

Tangent lineation diagrams

Tangent-lineation or slip-linear diagrams (Twiss and Gefell, 1990) offer a most effective means of analyzing kinematic data from faults, because they contain information about the orientation of the fault plane, as well as the orientation of the slip lineation. They are constructed by plotting the pole to each fault plane, and then aligning the pole and the lineation orientation on that plane; a short segment of a great circle is then drawn through the pole. This line then represents the 'M' or movement plane (after Arthaud, 1969), and is parallel to the instantaneous slip direction on the fault. An arrow on the M-plane shows the sense of movement of the hangingwall (Twiss and Gefell (1990) used the opposite convention). Both equal angle and equal area projections yield some distortion of the slip lineation relative to geographic coordinates, because of the combined use of poles to planes and angles between planes in this type of projection. Orthorhombic projections preserve the true slip-lineation direction relative to a geographic reference frame, but our data are presented using equal angle projections because the orthorhombic projections do not

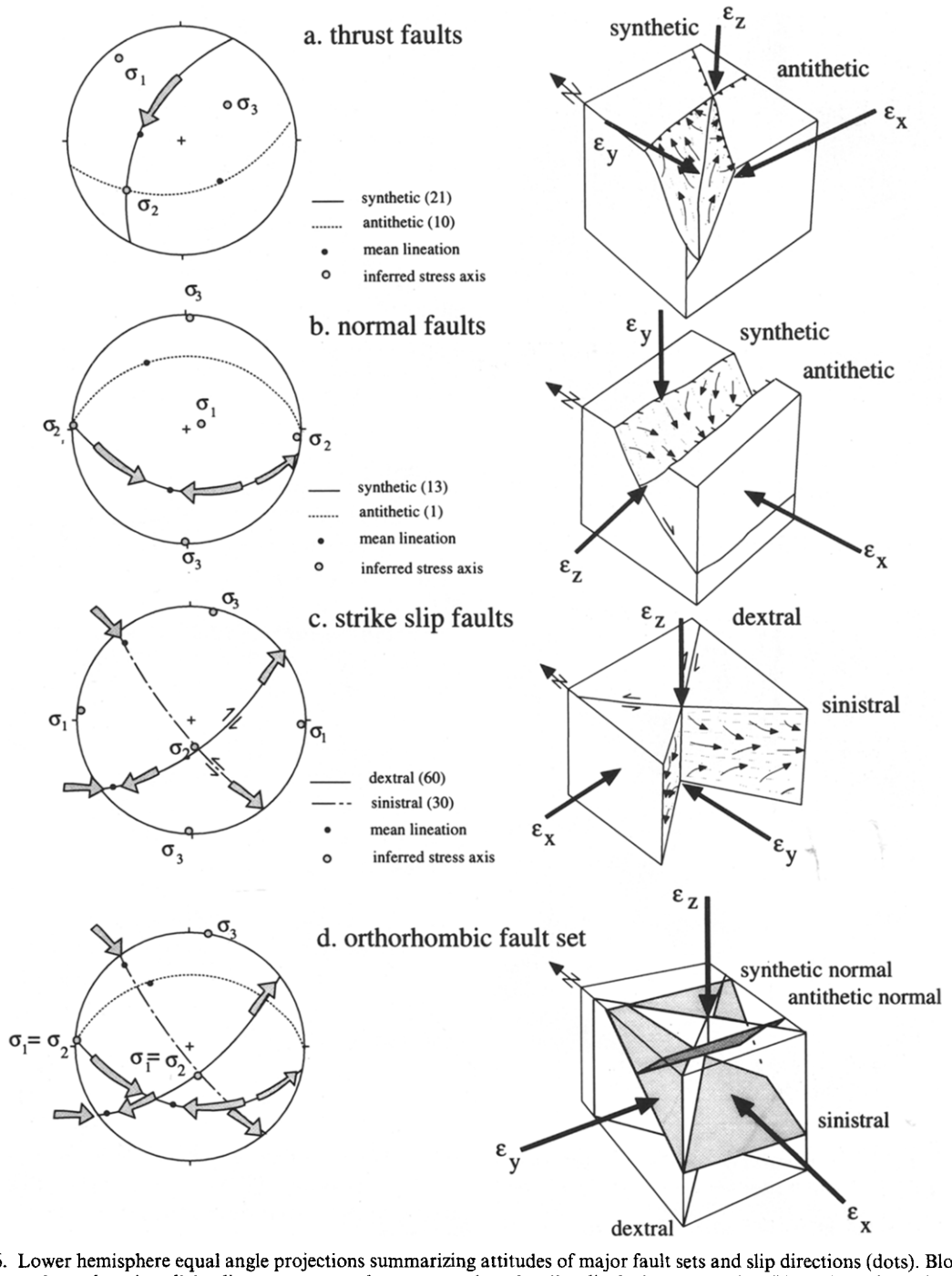

Fig. 6. Lower hemisphere equal angle projections summarizing attitudes of major fault sets and slip directions (dots). Block diagrams show changing slickenline patterns on thrust, normal, and strike-slip fault systems. (a), (b), and (c) show thrust, normal, and strike-slip fault systems, respectively, and (d) shows interpretation of normal plus strike-slip fault systems as an orthorhombic fault system. Equal angle projections also show stresses inferred from fault and slip-line orientations, whereas block diagrams show principal strains.

yield much separation of data near the edge of the net, such as poles to steep faults, which comprise a significant portion of the data set.

On tangent-lineation diagrams thrust faults plot as outward pointing slip-linears, with low-angle thrusts plotting in central parts of the net, and steep thrust faults plotting near the primitive circle. Purely dip-slip faults (with down- or up-dip lineations) plot as straight line segments of great circles, whereas oblique slip faults plot as curved great circle segments. Normal faults are similar, but show inward-pointing slip linears. Steep dextral and sinistral strike-slip faults plot near and parallel to the primitive circle, and have arrows pointing in a counterclockwise sense for dextral faults, and a clockwise sense for sinistral faults (note that the convention of Twiss and Gefell (1990), of plotting the arrowhead

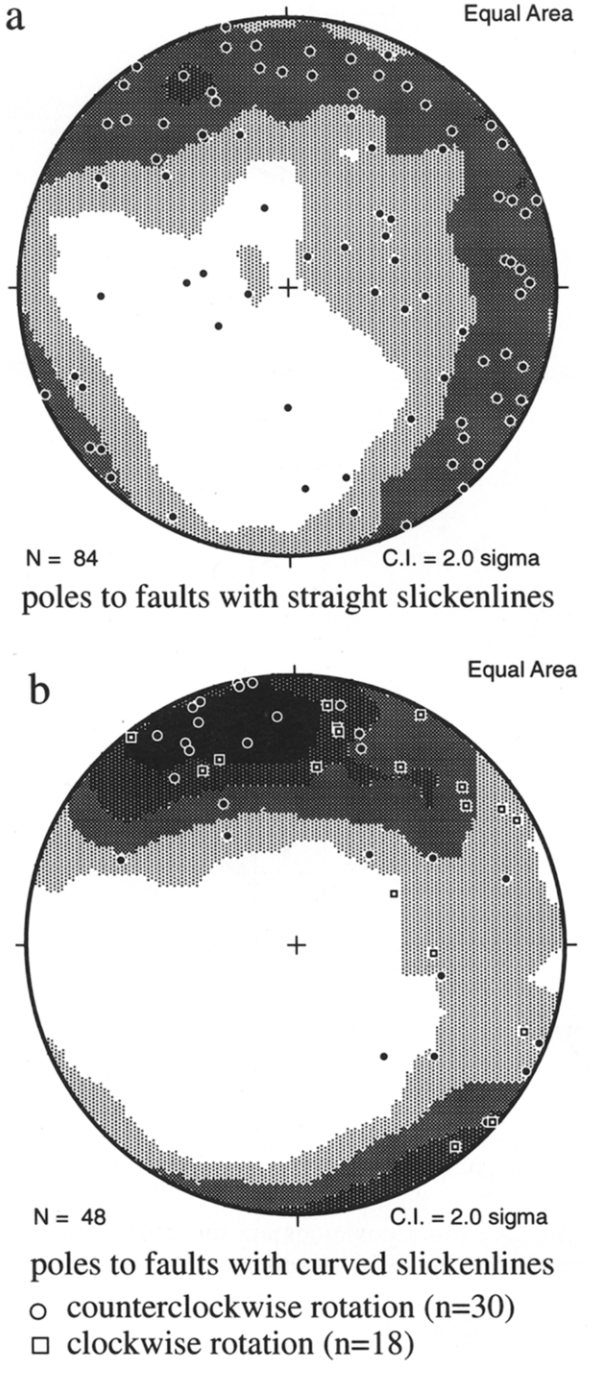

Fig. 7. Lower hemisphere equal area projections. (a) Poles to fault planes with straight slickenlines. Note abundance of faults that strike between 230° and 050°. (b) Poles to faults with curved slickenlines. Squares indicate slickenlines with clockwise curvature when viewed from above; dots, slickenlines with counterclockwise curvature when viewed from above. Note absence of faults that strike between 230° and 050°.

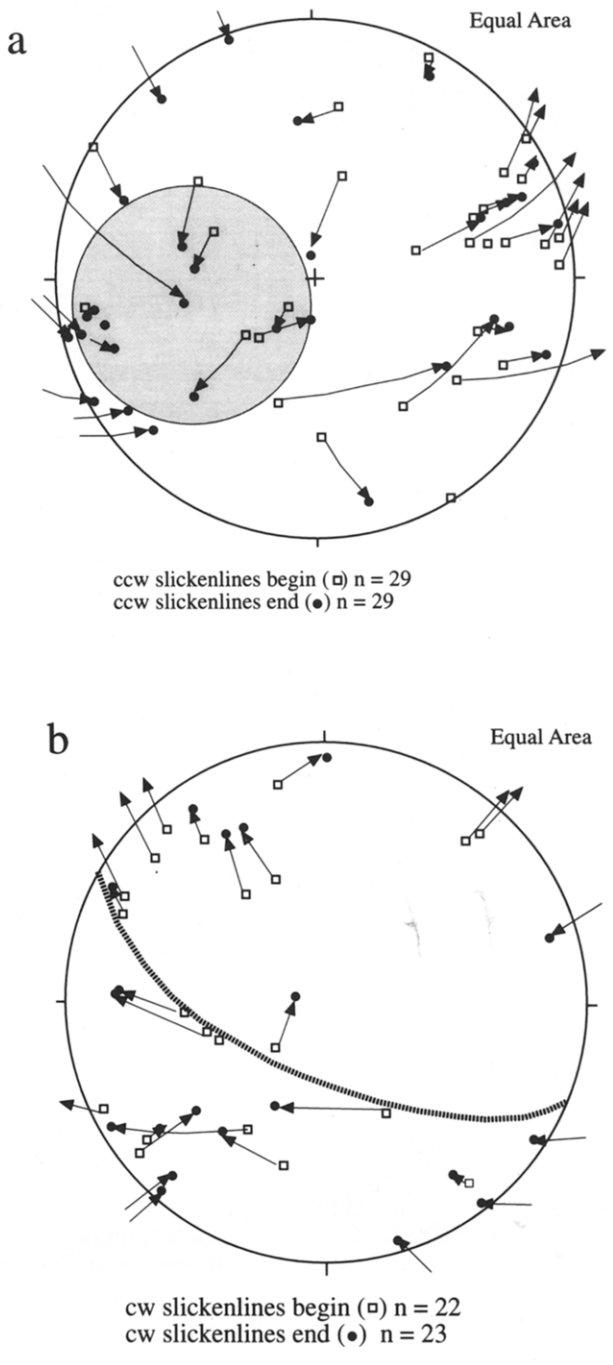

Fig. 8. Lower hemisphere equal area projections showing changes in trend and plunge of slickenfibers with (a) counterclockwise and (b) clockwise curvature. Arrows connect initial and final slickenfiber orientations (with arrowheads pointing to final orientation), but are not pointing in the slip directions. Gray area in (a) shows area where counterclockwise slickenlines are converging, and great circle in (b) shows girdle that clockwise slickenlines are diverging from.

for the footwall as opposed to the hangingwall, would yield the opposite curvature). Faults that have mixed or oblique-slip components (e.g. dextral thrust) will have tangent-lineation characteristics representing the proportional amount of each slip component, and are thus easier to interpret than conventional plots.

Figure 10 shows tangent lineation-diagrams for faults that have curved slickenfibers. In all plots, the solid line represents the final or last slip increment, whereas the dashed line represents the first recorded slip direction. We use these diagrams to determine whether with time, slip on the faults tended to become more or less Andersonian (i.e. more or less compatible with stress systems with one vertical principal stress), by determining whether the slip lineations are closer to or farther from being tangent to the primitive circle for strike-slip faults, and closer or

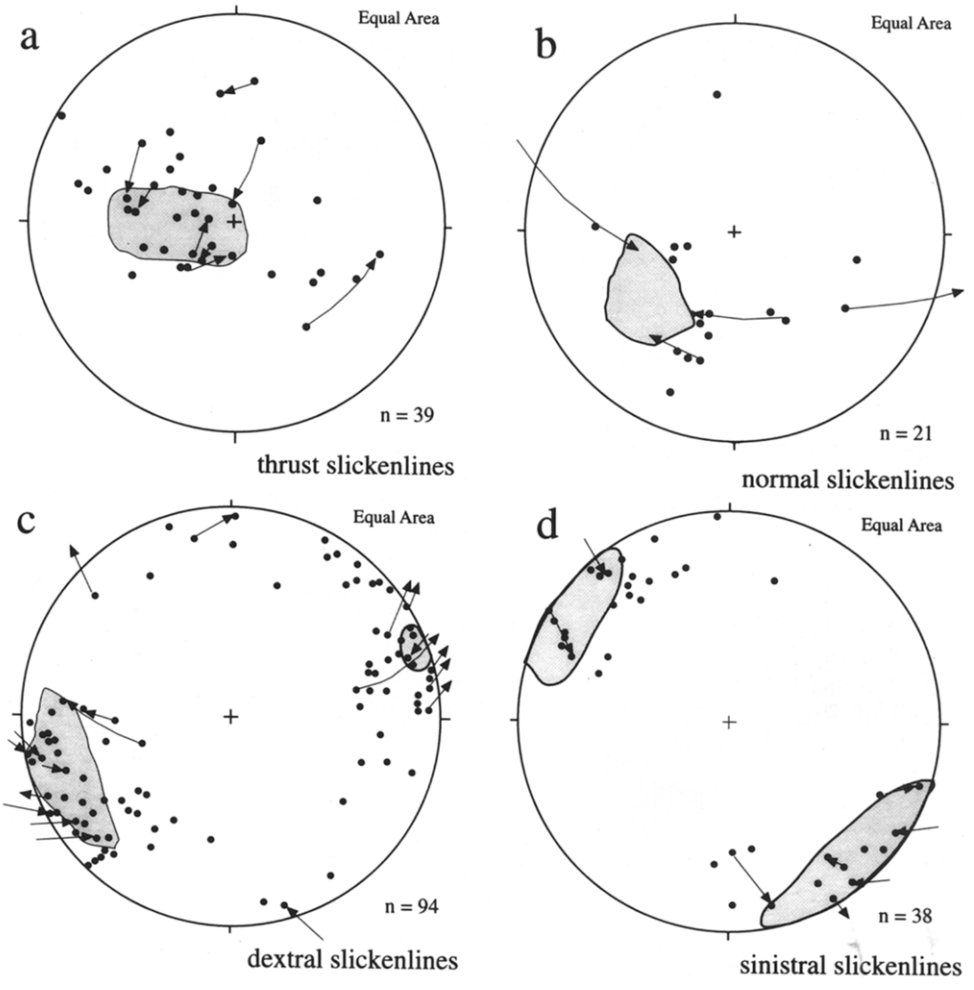

Fig. 9. Lower hemisphere equal area projections showing thrust (a), normal (b), sinistral (c) and dextral (d) slickenfibers, with arrows showing progressive changes in trend and plunge of curved slickenfibers. Gray areas show zones that curved fiber slip directions appear to be converging towards.

farther from being tangent to the radial slip lines for dip-slip faults. Figure 10 shows this by plotting tangent lineations that become more Andersonian with a (+) value, and those that become less Andersonian with a (−) value. The sense and amount of change of the slip lines are strongly biased, with 67% (72% if only the orthorhombic faults are used) of the cumulative rotations tending toward a more Andersonian system with younger slip increments. Thus, oblique dip-slip faults have a tendency to become more dip-slip with time, whereas oblique strike-slip faults tend to become pure strike-slip faults with younger slip increments.

INTERPRETATION: MULTIPLE FAULT SETS AND CURVED SLICKENLINES

Although Andersonian fault geometries successfully explain systems of conjugate faults formed under plane strain conditions, general, three-dimensional deformations require more complex fault configurations. In many cases, field geologists have interpreted multiple fault sets in terms of multiple deformation events. However, Reches (1978, 1983), Reches and Dieterich (1983), Krantz (1988, 1989) and Yin and Ranalli (1992) have shown that multiple fault sets with orthorhombic symmetry can accommodate a single three-dimensional strain. Four sets of faults minimize dissipation and form at the lowest differential stress (Reches, 1983). Reches (1978, 1983) and Krantz (1988) proposed slip models for orthorhombic fault systems in terms of irrotational strains, in which fault geometry is determined by the ratios of the principal strains.

In general, most faults preserve slip lineations that are roughly parallel for each successive strain increment. Mechanical interactions between faults, and changes in fault shape, or differences in frictional anisotropy along a single fault can all cause variations in slip directions along a single fault (Pollard *et al.*, 1993; Wojtal, 1996). In this contribution, we discuss variations in slip directions in time from single locations on individual faults. For these cases, the orientations of slip lineations may change if any one of several common phenomena occur. The hangingwall of the fault may simply rotate with respect to the footwall about an axis normal to the fault plane, or there may be an incremental change in slip direction

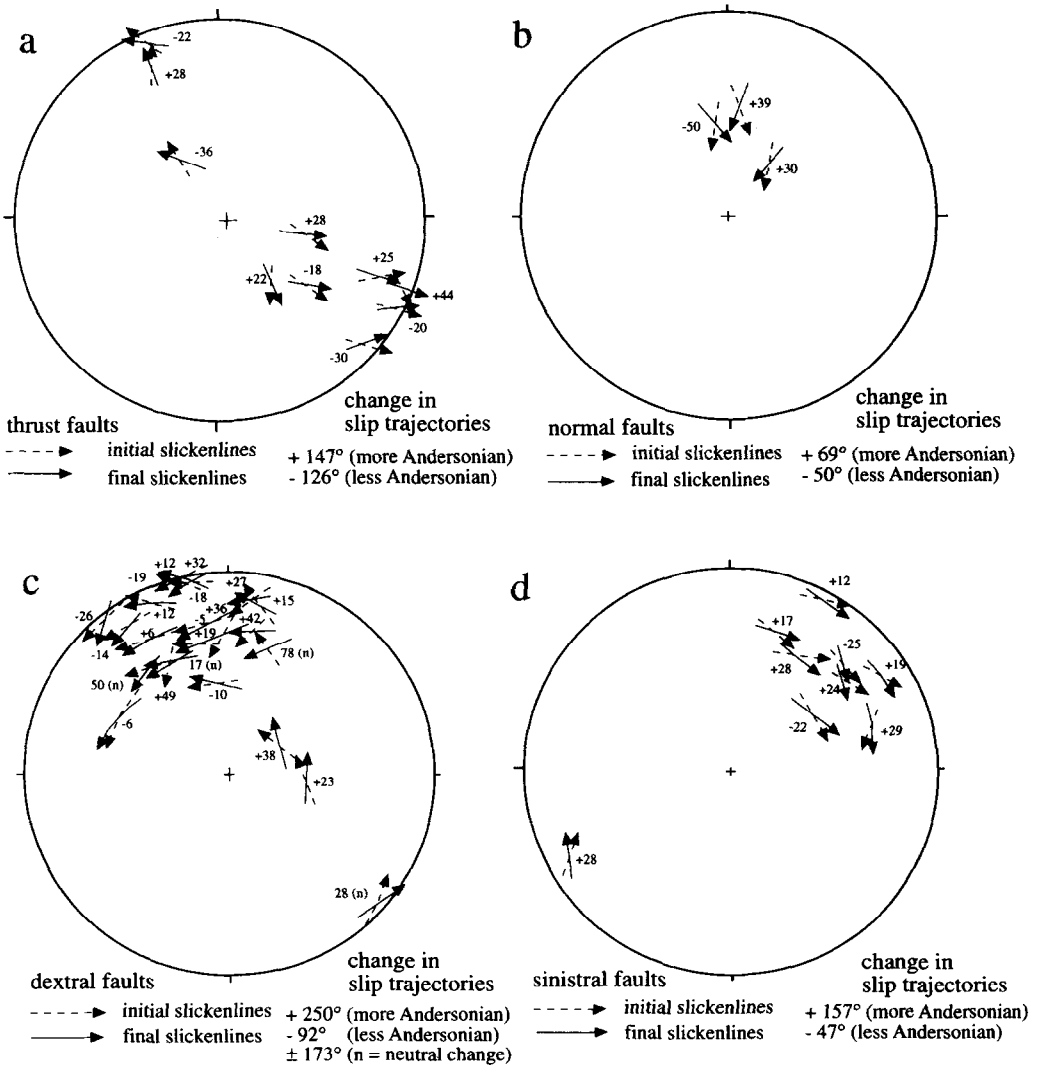

Fig. 10. Lower hemisphere equal area projections showing tangent lineation diagrams for the Turnagain Arm fault data. (a) Thrust fault data. (b) Normal fault data. (c) Dextral fault data. (d) Sinistral fault data. Numbers next to each pair of arrowheads shows angular change in slip linears, and sense (+) toward becoming more Andersonian, or (−) becoming less Andersonian with younger slip increments.

during each slip increment (rotational-translational motion and curvilinear-translational motion, respectively, of Mandal and Chakraborty, 1989). Changing ratios between principal stresses can cause a progressive fanning of slip-lineation orientations; for instance, unroofing will cause a progressive up-dip rotation of slip-lineations on thrust faults (Wilkerson and Marshak, 1991). Twiss and Gefell (1990) and Twiss *et al.* (1991) theorized that curved slickenline patterns on multiple fault sets form when the deforming rock mass consists of numerous small microblocks, each of which possesses a 'microspin' component of deformation that may be oblique to, but helps accommodate, the overall regional deformation.

Interpretation of curvature of slip lineations

The foregoing analysis shows that the rotation of slip directions on the orthorhombic fault set along Turnagain Arm was systematic, with slip on dip-slip faults tending to become steeper with younger slip increments and slip directions on strike-slip faults becoming shallower with time (Fig. 11). One possible explanation for this trend is that the stress system showed a tendency to go from non-Andersonian (with no vertical principal axes) to a more nearly Andersonian stress system (with one vertical principal stress) with time. The earliest formed lineations reveal that most fault sets began as oblique-slip systems, and gradually evolved into nearly dip-slip and strike-slip systems. Such a phenomenon might occur if a body of rocks were progressively unroofed* during the slip history of the fault systems (Wilkerson and Marshak, 1991). The slip lineations along Turnagain Arm may thus indicate progressive exhumation of the area during

*We use the term uplift to denote vertical movement relative to the geoid, and exhumation/unroofing to denote vertical movements relative to the erosional surface.

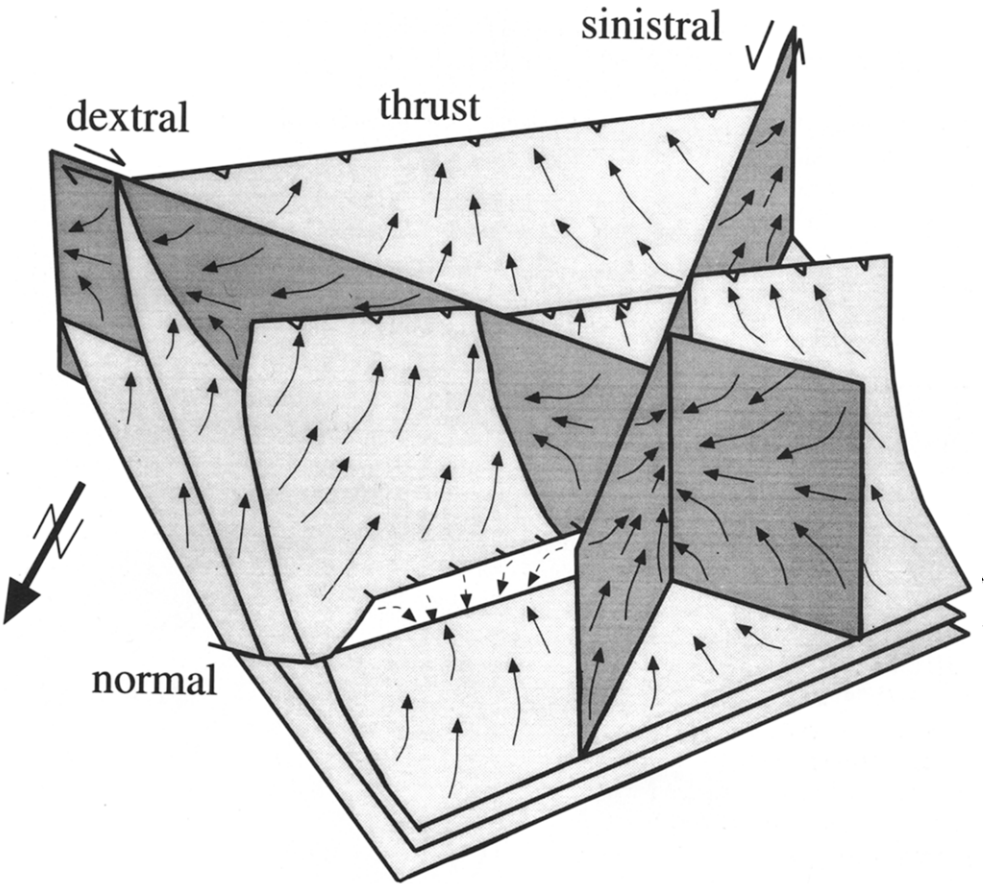

Fig. 11. Schematic block diagram of frontal pan of an accretionary wedge, showing changes in displacement directions on multiple faults.

deformation, and movement into an Andersonian stress field.

Assuming that the foregoing analysis of the timing of late thrust-, normal-, and strike-slip faults is correct, the stress system can be interpreted to reflect an early, gently northwestward plunging σ_1, southwest plunging σ_2, and northeast plunging σ_3. During formation of the late normal and strike-slip faults of the orthorhombic system, the slip-lineations converge on a configuration including nearly vertical σ_1 or σ_2 with nearly equal magnitudes, and an approximately horizontal σ_3, trending N–S (Fig. 6). These results suggest that σ_1 rotated from a gently inclined northwest direction during pre-ridge subduction plate interactions, to a horizontal E–W plunge after passage of the triple junction.

REGIONAL EXTENT OF ORTHORHOMBIC FAULT SETS

Late brittle faults like those along Turnagain Arm are widespread in the arc–trench gap of south-central Alaska. Bradley and Kusky (1992) recognized six subsets of late faults on the southern Kenai Peninsula (Fig. 2), including: (1) ENE-striking dextral faults; (2) NNW-striking sinistral faults; (3) N-striking dextral faults; (4) N-striking, W-dipping late thrusts; and (5) and (6) E-striking N- and S-dipping normal faults.

Similar sets of late faults occur on the outer coast of the Kenai Peninsula, including the area between the Nuka pluton, Resurrection Peninsula ophiolite, and the Nellie Juan and Eshamy plutons (Fig. 2). The Nuka pluton (56 ± 0.5 Ma, U/Pb on monazite; Bradley *et al.*, 1993) truncates early, NNW-striking normal faults, but is cut by an orthorhombic fault set consisting: of (1) NE-striking normal faults; (2) NE-striking thrust faults; (3) NW-striking sinistral faults; and (4) ENE-striking dextral faults. Slickenlines on the sinistral faults show changing displacement directions with progressive slip increments, beginning with oblique slip trajectories, and tending toward purely strike-slip displacements with age.

The pattern of faulting along Turnagain Arm is also similar to that described in the Paleocene Ghost Rocks Formation on southern Kodiak Island (Fig. 1), where Byrne (1984, 1986) reported the following sequence of late faults: (1) a conjugate pair of E-striking dextral and N-striking sinistral strike-slip faults; (2) a conjugate pair of NW-dipping synthetic and minor SE-dipping antithetic thrusts; and (3) a conjugate pair of E-striking normal faults. Each fault set on southern Kodiak Island

appears to have its counterpart along Turnagain Arm; orientations differ slightly but the overall configurations are similar.

On Afognak Island and northern Kodiak Island (Fig. 1), Sample and Moore (1987) identified a comparable system of late faults cutting the Upper Cretaceous Kodiak Formation (the along-strike correlative of the Valdez Group): (1) NE-striking, dextral, strike-slip faults (conjugate sinistral faults were not reported); (2) NW-dipping thrusts; and (3) normal faults with highly variable strikes. The relative age of these three fault sets is unknown, but like the Turnagain Arm faults, they postdate penetrative deformation.

Late faults with curved calcite–chlorite slickenfibers are also abundant in the northern Chugach mountains (T. Kusky and G. Plafker, 1996, unpubl. field notes), and V.B. Sisson (pers. comm., 1992) has reported that late-stage faults are extremely abundant in the Chugach metamorphic complex, north of the Yakutat terrane (Fig. 1), but these structures have yet to be systematically analyzed. Haeussler *et al.* (1994) described numerous brittle faults in the Chichagof and Baranof Islands in southeastern Alaska, and noted that these are nearly all NW-striking dextral, strike-slip faults. Whereas more data are needed to clarify the regional pattern and kinematics of late faulting, the available data confirm that late brittle faults are widespread along a 2000 km long segment of the accretionary wedge.

TIMING OF LATE FAULTS

Two independent lines of evidence indicate that faulting occurred in the Paleogene, in association with passage of the Kula–Farallon–North America triple junction: (1) some correlative strike-slip faults on the southern Kenai Peninsula exhibit mutually cross-cutting relationships with igneous dikes dated at 54–57 Ma (Bradley *et al.*, 1994), constraining the timing of movement on the strike-slip faults; and (2) correlative faults of the strike-slip and normal sets are locally mineralized, and the gold mineralization is also dated at 53–57 Ma in Kenai Peninsula and the Girdwood area (Haeussler *et al.*, 1995).

Contemporaneity with near-trench magmatism

Field relationships that most convincingly document the contemporaneity of dikes and faults, are mapped at the toe of Grewingk Glacier, east of Kachemack Bay (Figs 3 & 12). Here, several mafic dikes intrude along NE-striking dextral faults (marking the contact between cherty argillite and greenstone in Fig. 12a) which provided the zones of weakness along which dikes were intruded. Thin dextral fault zones occur near the centers of the dikes (Fig. 12a), suggesting that faulting and diking were contemporaneous. In other places, the NE-striking dextral faults clearly cut mafic dikes, incorporating fragments of the dikes in the fault breccia (Fig. 12b). We interpret these mutually cross-cutting relationships to indicate that at Grewingk glacier, late dextral faulting was broadly contemporaneous with intrusion of the intermediate dikes. All intrusions in this area have 54–57 Ma ages (the time of inferred ridge subduction; Bradley *et al.*, 1994), linking the late faulting with the ridge subduction process.

Contemporaneity with gold veins

Structural and geochronological data from gold-mineralized late faults in the Chugach and Kenai Mountains help constrain the timing of late faulting in the Chugach terrane. Gold veins are found chiefly within the Valdez Group, but also within the McHugh Complex and Orca Group (Goldfarb *et al.*, 1986). Many of the gold–quartz veins are spatially associated with Paleocene–Eocene near-trench granitic intrusives, but in all cases where both occur, the veins are clearly younger than the intrusions (Haeussler and Bradley, 1993). The gold–quartz veins occur in steeply-dipping faults and fractures filled with mineral phases (quartz, less commonly calcite, minor chlorite) and wall-rock fragments very similar to the faults along Turnagain Arm (Mitchell, 1979; Pickthorn, 1982; Stuwe, 1986; Hoekzema *et al.*, 1987; Haeussler and Bradley, 1993). The mined gold–quartz veins were up to about 1.5 m in width. This is wider than the faults along Turnagain Arm, but this may be due to the fact that structures along which there is preferential fluid flow would also be favorable to gold deposition. A compilation of structural data from these mines and prospects (Haeussler and Bradley, 1993, 1996; Haeussler *et al.*, 1995) suggests that the structures along which gold-bearing quartz veins occur are structurally and texturally identical to the fault sets along Turnagain Arm. The mineralized structures are always strike-slip and normal faults; no evidence exists for gold mineralization on thrust faults. Because both the Turnagain Arm fault sets and the structures hosting gold veins in the Chugach and Kenai Mountains have the same structural style, same fault/vein mineralogy, and the same cross-cutting relationships, it very likely that both formed from similar processes. A gold–quartz vein located 15 km north of Turnagain Arm in the Girdwood district (Fig. 4), yielded a $^{40}Ar/^{39}Ar$ age on white mica of 54.3 ± 0.1 Ma (Haeussler *et al.*, 1995). A hydrothermally altered and mineralized dike located 10 km southwest of Turnagain Arm in the Hope-Sunrise district (Fig. 3), yielded K–Ar dates similar to the higher quality $^{40}Ar/^{39}Ar$ date from the Girdwood area (52.7 ± 1.6 Ma-whole rock, and 53.2 ± 1.6 Ma-white mica; Silberman *et al.*, 1981). Therefore, brittle faulting along Turnagain Arm also likely occurred around 54 Ma.

Mounting geochronological evidence exists for gold mineralization having been related to the Paleocene and Eocene episode of ridge subduction beneath southern Alaska. Bradley *et al.* (1993) have shown that a

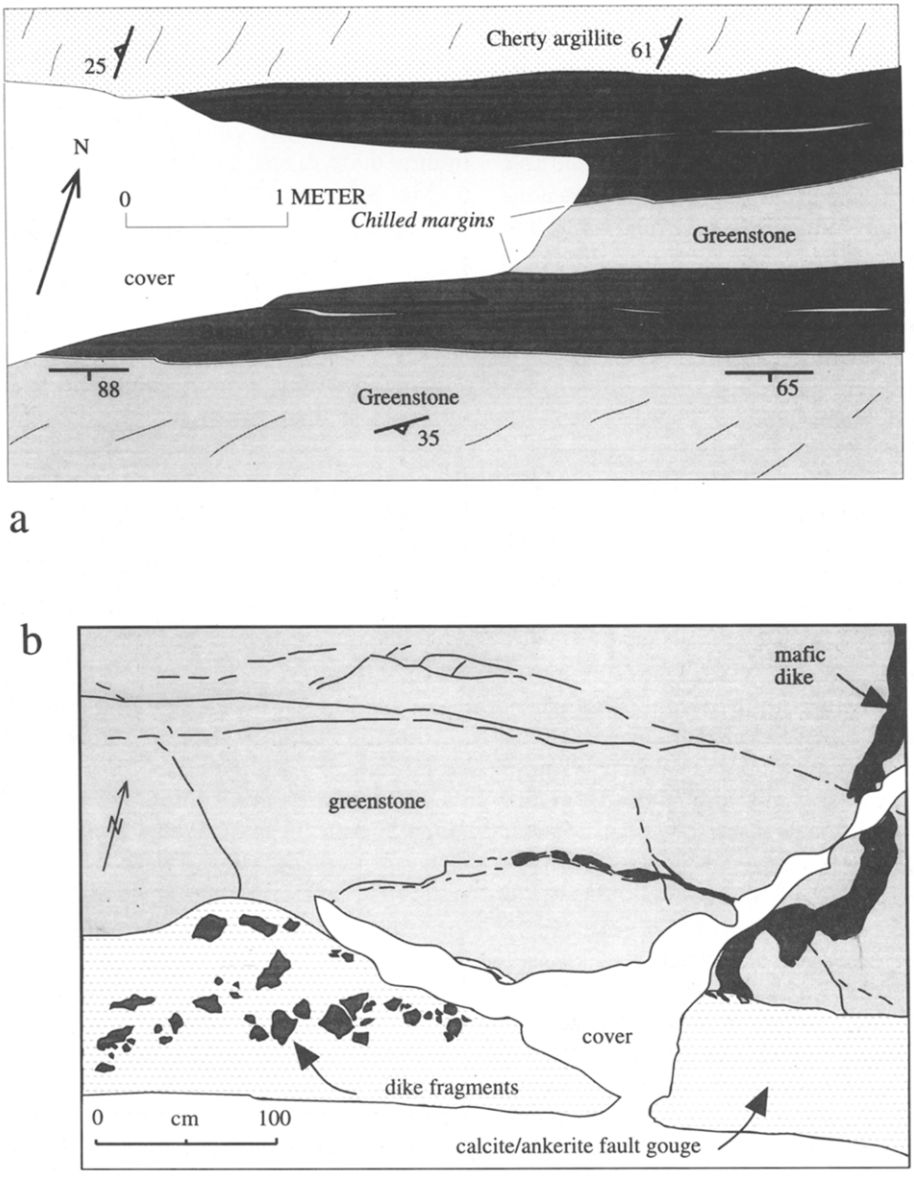

Fig. 12. Detailed maps from Grewingk Glacier (southern Kenai Peninsula; see Fig. 2 for location), showing mutually, cross-cutting relationships between late strike-slip faults and mafic to intermediate dikes. (a) Two dikes that are cut by dextral faults along the same fault zone a few hundred meters away, but here the dikes were intruded along the fault before the youngest increment of motion. (b) Field sketch of a dike cut by a dextral fault, with pieces of the dike incorporated into the fault breccia.

progression in ages of near-trench intrusions occurs in southern Alaska from older (63–65 Ma) in the west to younger (50 Ma) in the east. Haeussler *et al.* (1995) have shown from $^{40}Ar/^{39}Ar$ dating of micas from gold–quartz veins that the ages of gold–quartz veins are very similar to, and within 0.9 Ma of, the age of nearby well-dated near-trench intrusions. In addition, gold mineralization shows the same diachronous age pattern as the ages of near-trench intrusions, suggesting the gold mineralization is related to the ridge subduction process (Haeussler *et al.*, 1995). Therefore, because the structures that host the gold are very similar to the late faults it is likely that the late faults are also related to ridge subduction.

The lack of gold mineralization on thrust faults suggests that they are slightly older than the strike-slip and normal faults. Several cross-cutting relationships on the faults along Turnagain Arm and on the Kenai Peninsula indicate that thrusts may be older structures. In addition, the misorientation of thrusts with respect to the other fault sets suggests there is a slight difference in their age.

TECTONIC SIGNIFICANCE

The orthorhombic faults examined in this study formed late in the structural evolution of the southern Alaska accretionary wedge because they cut mélange fabrics and slaty cleavage related to offscraping/underplating. To understand what caused the faults, this section examines the late, post-accretion tectonic history of the southern Alaska convergent margin. Potentially

important processes and events include: (1) critical taper adjustments of the accretionary wedge in response to continued underplating and outboard accretion; (2) major orogen-parallel strike-slip; (3) formation of the southern Alaska orocline; and (4) subduction of the Kula–Farallon ridge. Since the structures are distinctly diachronous along strike, and associated with a migrating thermal and magmatic pulse, we can eliminate mechanisms (1), (2), and (3), and focus on mechanical responses of the wedge to ridge subduction as a causal mechanism for the late faulting event.

Triple junction effects

Subduction of the Kula–Farallon ridge in early Tertiary time, with associated migration of the Kula–Farallon–North America triple junction had profound effects on the tectonics of the Cordillera (Byrne, 1979; Stock and Molnar, 1988; Bradley *et al.*, 1993; Sisson and Pavlis, 1993; Harris *et al.*, 1996). We explore the hypothesis that at least some of the strain recorded by the late faults is related to triple-junction tectonics. One possibility is that the faults formed in response to subduction of the topographically high-standing Kula–Farallon ridge, and reflect uplift and exhumation of deeper levels of the accretionary prism in response to this event. Models of accretionary wedge mechanics (Chapple, 1978; Davis *et al.*, 1983; Dahlen *et al.*, 1984; Platt, 1986; Fletcher, 1989) predict that when the dip of the basal décollement decreases, such as when younger-age crust approaches the trench preceding ridge subduction, that the wedge should respond by internally contracting, to maintain the critical taper (basal dip plus surface slope). After the triple junction passes, progressively older lithosphere will be subducted, with consequent steeper dips of the basal décollement. At this point the wedge will recover its lower surface slope, perhaps through normal faulting. An additional but related complexity is that the late faults may also reflect changes in the obliquity of convergence, as different plates with different convergence vectors are subducted before and after triple junction migration through a region.

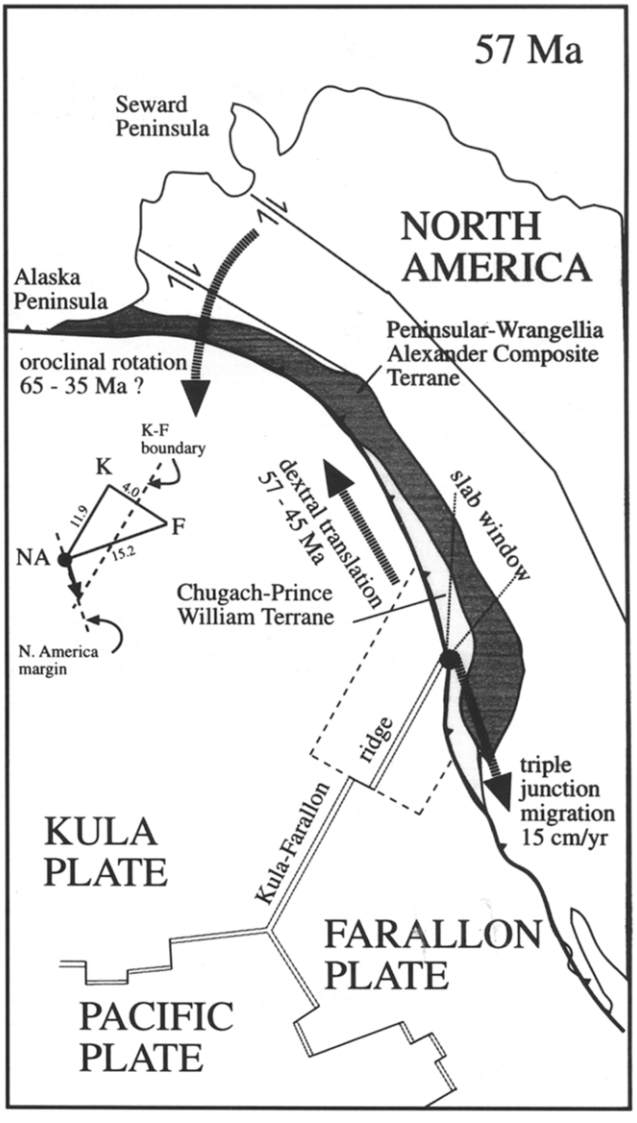

Fig. 13. Eocene plate reconstruction of the North Pacific and North American cordillera showing location of the Kula–Farallon–North America triple junction, and its southward migration of 15 cm a^{-1}. Based in part on Bol *et al.* (1992), Engebretson *et al.* (1985), Lonsdale (1988), Sisson and Pavlis (1993), and Bradley *et al.* (1994).

These altemative but related possibilities are illustrated in Figs 13 and 14. Parts of the wedge that have not yet experienced ridge subduction will be progressively uplifted on the flanks of the approaching ridge, perhaps causing increased horizontal contraction and vertical extension of the wedge. Thrust faults formed at this time will have orientations related to the slope of the surface of the wedge, and the basal décollement, as in other thrust wedges and accretionary prisms (Chapple, 1978; Davis *et al.*, 1983; Dahlen *et al.*, 1984). Along Turnagain Arm, the orientation of the late thrusts may have been significantly affected by pre-existing anisotropies. Other structures in the wedge may have orientations and kinematics reflecting relative convergence vectors between the Farallon and North America plates (Fig. 13, plates B and C in Fig. 14), which according to vector triangles based on North Pacific plate reconstructions (Engebretson *et al.*, 1985; Lonsdale, 1988; Sisson and Pavlis, 1993) was nearly orthogonal convergence prior to ridge subduction. After the triple junction passes, structures in the wedge related to surface forces will reflect convergence between the Kula and North American plates (Fig. 13, plates A and C in Fig. 14), which was dextral oblique convergence after triple junction migration (see vector triangles in Figs 13 & 14). As the accretionary prism rides down the passing flank of the subducting ridge (Fig. 14), the dip of the basal décollement will increase. Much of the horizontal extension of the wedge, at an angle to orogenic strike, was accomplished at this stage along the normal and strike-slip faults, and the evidence from the southern Kenai Peninsula shows that these sets of faults were active

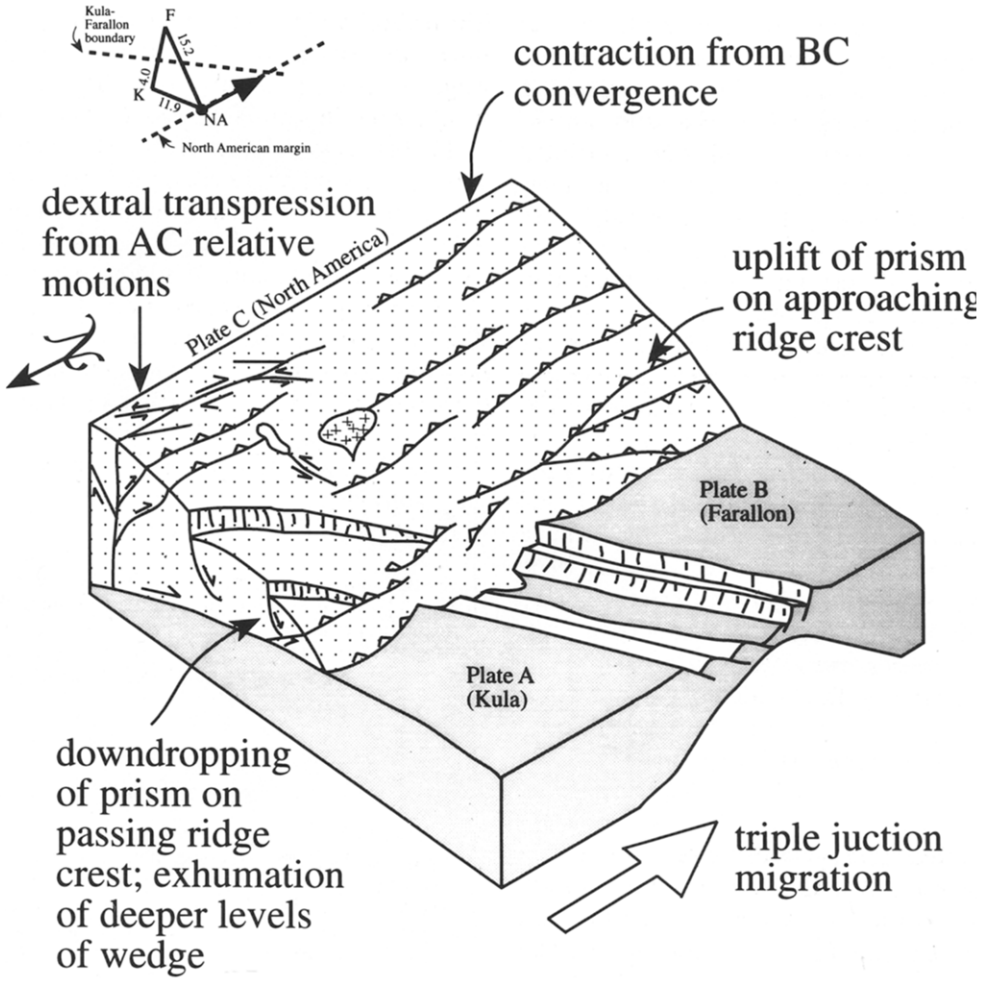

Fig. 14. Possible relationship of late faults to ridge subduction. See text for explanation.

during emplacement of dikes and gold–quartz veins associated with passage of the triple junction. We speculate that the orientation of the extensional axis may reflect the orientation of the down-going ridge (Fig. 14), but the regional orientation of dikes is too variable to propose a more detailed model at this stage. Some of these structures may be normal faults transferred from block faults on down-going ridge crest to rotational-normal faults in the over-riding wedge, and others may reflect extension parallel to topography of the down-going ridge crest along the thermal conductive cooling curve.

If the late faults formed in response to subduction of the high-standing ridge, they could accommodate instantaneous critical taper adjustments of the wedge, and the structures would be short-lived and distinctly diachronous along strike, forming at the same as time, or shortly after, near-trench intrusives related to ridge subduction (Bradley *et al.*, 1993). This prediction is supported by the diachronous ages of faulting obtained by dating syn-faulting gold–sericite veins, as described above. Conversely, if the late faults are a response to changes in the stress configuration in the wedge after migration of the triple junction, then the time at which the fault system formed or changed its slip directions should be diachronous along strike, but the faults would continue to be active for some time, and the same fault systems could be active in different locations in the wedge at the same time, as long as all locations were located on the same side of the triple junction. Current data (Fig. 1c) suggests that the late faulting event was short lived, supporting the idea that the faults represent instantaneous critical taper adjustments of the wedge in response to ridge subduction.

Relationship of late faults to orogen-parallel strike-slip

The southern Alaska convergent margin was affected by major strike-slip translations along the continental margin during and after individual thrust packages of the Chugach terrane were scraped off oceanic plates of the Pacific basin (Engebretson *et al.*, 1984, 1985; Stock and Molnar, 1988; Atwater, 1989). Bol *et al.* (1992) suggest $13 \pm 7°$ of northward motion of the Resurrection Peninsula ophiolite within Chugach Terrane since about 57 Ma. The late fault sets along Turnagain Arm record shortening perpendicular to the trench, and extension

along strike, and we cannot directly relate the late thrust or the orthorhombic fault systems to this tectonic event. Furthermore, gold mineralization along these faults is distinctly diachronous along-strike (Haeussler *et al.*, 1993). However, the very late gouge-filled NNE-striking dextral strike-slip faults that cut faults of the orthorhombic fault set may have formed during this event. These youngest dextral-faults, however, are minor structures incapable of accommodating major plate motions, and most of the major orogen-parallel strike-slip motions must have been accommodated along other major structures such as the Border Ranges fault zone (Little and Naeser, 1989; Little, 1990; Roeske *et al.*, 1993). The Border Ranges fault forms the boundary between the Wrangellia and Chugach–Prince William superterranes; it initiated as a subduction thrust (MacKevett and Plafker, 1974) but was reactivated in various places as a strike-slip or normal fault (Pavlis and Crouse, 1989; Little and Naeser, 1989; Little, 1990; Roeske *et al.*, 1991). There is however, little geologic data supporting large strike-slip displacements even on these major faults (Nokleberg *et al.*, 1989; Plafker *et al.*, 1989).

Modern analogs: subduction of the Cocos–Nazca ridge, and Nazca ridge

Subduction of the Cocos–Nazca ridge and Panama fracture zone in Central America offers a modern analog for the sequence of structures preserved in the southern Alaska accretionary prism. Heil (1988) documented that as the ridge approaches the accretionary prism, the wedge contracts, forming re-entrants and thrust faults, which rotate into parallelism with the down-going ridge as the thrusts encounter thinner sediments on the ridge flanks. This is associated with an increase in the critical taper of the wedge, and increased thrust faulting immediately preceding collision of the ridge. After passage of the fracture-zone ridge, the accretionary wedge rides on a progressively steepening subducting plate, and the wedge gradually recovers its pre-collision taper, possibly through extensional faulting (Heil, 1988). Hsu (1992) examined Quaternary and late Pliocene (?) marine terraces in the vicinity of the Nazca ridge along the Peruvian coast. He found the topography of the terraces mimicks the topography of the Nazca ridge, and that the highest rates of uplift are on the side of the ridge that the ridge is moving towards. This sequence of structures and uplift history is remarkably similar to that documented here for the Chugach accretionary prism, suggesting a common structural response to subduction of topographically high standing objects.

CONCLUSIONS

The Chugach terrane of south central Alaska is cut by abundant late faults that progress from thrusts to an orthorhombic system of strike-slip and normal faults. The orthorhombic faults are the same age as near-trench intrusives related to subduction of the Kula–Farallon ridge in the Paleogene, that show an along strike progression in age, from 65–63 Ma in the west, to 50 Ma in the east. The late fault system records a complex kinematic evolution, including an early oblique-slip subhorizontal σ_1, associated with thrust faulting, and shortening of the wedge over the shallowing dip of the progressively younging Farallon plate as the Kula–Farallon ridge approached. Late dextral and sinistral faults are contemporaneous with near-trench intrusives, and record subvertical $\sigma_1 = \sigma_2$, associated with oblique extension of the wedge, after passage of the triple junction. A new kinematic regime followed, including dextral strike-slip faulting and translation of the Chugach terrane along the Cordilleran margin above the obliquely subducting Kula plate.

Acknowledgements—This manuscript has been improved by reviews from Sarah Roeske, Warren Nokleberg, Steve Wojtal, and an anonymous reviewer. Structural data is plotted using the stereonet program of Rick Almendinger. Supported by NSF EAR 9304647, awarded to T. Kusky, and by the United States Geological Survey.

REFERENCES

Arthaud, F. (1969) Methode de determination graphique des directions de raccourcissement, d'allongement et intermediare d'une population de failles. *Bulletin de la Société geologique de France* **11**, 729–737.

Atwater, T. (1989) Plate tectonic history of the northeast Pacific and western North America. In *The Geology of North America, N: The Eastern Pacific Ocean and Hawaii*, eds E. L. Winterer, D. M. Hussong and R. W. Decker. Geological Society America Press, Denver, 1–39.

Bol, A., Coe, R. S., Gromme, C. S. and Hillhouse, J. W. (1992) Paleomagnetism of the Resurrection Peninsula, Alaska: Implications for the tectonics of southern Alaska and the Kula–Farallon ridge. *Journal of geophysical Research* **97**, 17,213–17,232.

Bradley, D. C., Haeussler, P. J. and Kusky T. M. (1993) Timing of Early Tertiary ridge subduction in southern Alaska. In *Geologic Studies in Alaska by the U.S.G.S. during 1992*, ed. A. Till. *Bulletin of U.S. geological Survey* **2068**, 163–177.

Bradley, D. C. and Kusky, T. M. (1990) Kinematics of late faults along Turnagain Arm, Mesozoic accretionary complex, south-central Alaska. In *Geologic Studies in Alaska by the U. S. Geological Survey, 1989*, eds J. H. Dover and J. P. Galloway. *Bulletin of U.S. geological Survey* **1946**, 3–10.

Bradley, D. C. and Kusky, T. M. (1992) Deformation history of the McHugh Complex, Seldovia Quadrangle, south-central Alaska. In *Geologic Studies in Alaska by the U.S. Geological Survey, 1990*, eds D. C. Bradley and A. Ford. *Bulletin of U.S. geological Survey* **1999**, 17–32.

Butler, R. W. H. (1982) The terminology of structures in thrust belts. *Journal of Structural Geology* **4**, 239–245.

Byrne, T. (1979) Late Paleocene demise of the Kula–Pacific spreading center. *Geology* **7**, 341–344.

Byrne, T. (1984) Early deformation in melange terranes of the Ghost Rocks Formation, Kodiak Islands Alaska. *Special Paper geological Society America* **198**, 21–51.

Byrne, T. (1986) Eocene underplating along the Kodiak shelf Alaska: Implications and regional correlations. *Tectonics* **5**, 403–421.

Chapple, W. M. (1978) Mechanics of thin-skinned fold-and-thrust belts. *Bulletin geological Society America* **89**, 1189–1198.

Clark, S. H. B. (1973) The McHugh Complex of south-central Alaska. *Bulletin of U.S. geological Survey* **1372-D**, D1–D11.

Cowan, D. S. (1985) Structural styles in Mesozoic and Cenozoic melanges in western Cordillera of North America. *Bulletin of geological Society America* **96**, 451–462.

Dahlen, F. A., Suppe, J. and Davis, D. (1984) Mechanics of fold-and-thrust belts and accretionary prisms: Cohesive Coulomb theory. *Journal of geophysical Research* **89**, 10,087–10,101.

Davis, D., Suppe, J. and Dahlen, F. A. (1983) Mechanics of fold-and-thrust belts and accretionary wedges. *Journal of geophysical Research* **88**, 1153–1172.

Dumoulin, J. A. (1987) Sandstone composition of the Valdez and Orca Groups, Prince William Sound, Alaska. *Bulletin of U.S. geological Survey* **1774**.

Engebretson, D. C., Cox, A. and Gordon, R. G. (1984) Relative motions between oceanic plates of the Pacific basin. *Journal of geophysical Research* **89**, 10,291–10,310.

Engebretson, D. C., Cox, A. and Gordon, R. G. (1985) Relative plate motions between oceanic and continental plates in the Pacific basin. *Special Paper geological Society America* **206**.

Fisher, D. and Byrne, T. (1987) Structural evolution of underthrusted sediments Kodiak islands, Alaska. *Tectonics* **6**, 775–793.

Fletcher, R. C. (1989) Approximate analytical solutions for a cohesive fold-and-thrust wedge: some results for lateral variations in wedge properties and for finite wedge angle. *Journal of geophysical Research* **94**, 10,347–10,354.

Goldfarb, R. J., Leach, D. L., Miller, M. L. and Pickthorn W. J. (1986) Geology, metamorphic setting, and genetic constrains of epigenetic lode-gold mineralization within the Cretaceous Valdez Group, south-central Alaska. In *Turbidite-hosted Gold Deposits*, eds J. D. Keppie, R. W. Boyle and S. J. Haynes. *Special Paper Geological Association Canada* **32**, 87–105.

Haeussler, P. J., Davis, J., Steven, Roeske, Sarah, M. and Karl, S. M. (1994) Late Mesozoic and Cenozoic faulting at the leading edge of North America, Chichagof and Baranof Islands, southeastern Alaska. *Geological Society America, Abstracts with Programs* **26**, A317.

Haeussler, P. J. and Nelson, S. W. (1993) Structural evolution of the Chugach–Prince William Terrane at the hinge of the orocline in Prince William Sound, and implications for ore deposits. In *Geologic Studies in Alaska by the U.S.G.S. in 1992*, eds C. Dusel-Bacon and A. B. Till. *Bulletin U.S. geological Survey* **2068**, 143–162.

Haeussler, P. J., Bradley, D. C., Goldfarb, R. J., Snee, L. and Taylor, C. (1995) A link between ridge subduction and gold mineralization in southern Alaska. *Geology* **23**, 995–998.

Haeussler, P. J. and Bradley, D. C. (1993) Map and compilation of structural data from lode-gold mineral occurrences in the Chugach–Prince William terrane of southern Alaska. *U.S. Geological Survey Open-File Report* **93-325**.

Haeussler, P. J. and Bradley, D. C. (1996) Structural characteristics of ridge-subduction related gold deposits in southern Alaska. *Geological Society America, Abstracts with Programs* **28**, 71–72.

Harris, N. R., Sisson, V. B., Wright, J. E. and Pavlis, T. L. (1996) Evidence for Eocene mafic underplating during fore-arc intrusive activity, eastern Chugach Mountains Alaska. *Geology* **24**, 263–266.

Heil, D. J. (1988) Response of an accretionary prism to transform ridge collision south of Panama. Unpublished M.Sc. Thesis, University of California, Santa Cruz.

Hill, M., Morris, J. and Whelan, J. (1981) Hybrid granodiorites intruding the accretionary prism, Kodiak, Shumagin, and Sanak Islands, southwest Alaska. *Journal of geophysical Research* **86**, 10,569–10,590.

Hoekzema, R. B., Fechner, S. A. and Kurtak, J. M. (1987) Evaluation of selected lode gold deposits in the Chugach National Forest, Alaska. *U.S. Bureau of Mines Information Circular* **9113**.

Hsu, J. T. (1992) Quaternary uplift of the Peruvian coast related to subduction of the Nazca ridge: 13.5 to 15.6 degrees south latitude. *Quaternary International* **15/16**, 87–97.

Hudson, T. (1979) Mesozoic plutonic belts of southern Alaska. *Geology* **7**, 230–234.

Hudson, T. (1983) Calc-alkaline plutonism along the Pacific rim of southern Alaska: Circum-Pacific Terranes. *Memoirs of geological Society America* **159**, 159–169.

Krantz, R. W. (1988) Multiple fault sets and three-dimensional strain: Theory and application. *Journal of Structural Geology* **10**, 225–237.

Krantz, R. W. (1989) Orthorhombic fault patterns: The odd axis model and slip vector orientations. *Tectonics* **8**, 483–495.

Kusky, T. M., Bradley, D. C., Haeussler, P. H., Karl, S. K. and Donley, D. T. (1993) The Chugach Bay thrust, a major tectonic boundary in the Seldovia Quadrangle, south-central Alaska. *Geological Society America, Abstracts with Programs* **25**, 282.

Little, T. A. (1990) Kinematics of wrench and divergent-wrench deformation along a central part of the Border Ranges Fault system, northern Chugach Mountains Alaska. *Tectonics* **9**, 585–611.

Little, T. A. and Naeser, C. W. (1989) Tertiary tectonics of the Border Ranges Fault system, Chugach Mountains, Alaska; Deformation and uplift in a forearc setting. *Journal of geophysical Research* **94**, 4333–4359.

Lonsdale, P. (1988) Paleogene history of the Kula plate: Offshore evidence and onshore implications. *Bulletin of geological Society America* **100**, 733–754.

MacKevett, E. M. and Plafker, G. (1974) The Border Ranges fault in south-central Alaska. *Journal of Research of the U.S. geological Survey* **2**, 323–329.

Magoon, L. B., Adkison, W. L. and Egbert, R. M. (1976) Map showing geology, wildcat wells, Tertiary plant fossil localities, K–Ar age dates, and petroleum operations, Cook Inlet area, Alaska. *U.S. geological Survey Miscellaneous Investigations Series Map* I-1019, scale 1:250,000.

Mandal, N. and Chakraborty, C. (1989) Fault motion and curved slickenlines: A theoretical analysis. *Journal of Structural Geology* **11**, 497–501.

Marshak, R. S. and Karig, D. E. (1977) Triple junctions as the cause for anomalously near trench igneous activity between the trench and volcanic arc. *Geology* **5**, 233–236.

Mitchell, P. A. 1979. Geology of the Hope-Sunrise (gold) mining district, north-central Kenai Peninsula, Alaska. Unpublished M.S. thesis, Stanford University.

Nelson, S. W., Blome, C. D. and Karl, S. M. (1987) Late Triassic and Early Cretaceous fossil ages from the McHugh Complex, southern Alaska. *U.S. geological Survey Circular* **998**, 96–98.

Nilsen, T. and Zuffa, G. G. 1982. The Chugach Terrane, a Cretaceous trench-fill deposit, southern Alaska. In *Trench–Forearc Geology*, ed. J. K. Leggett. Blackwell Scientific, London, 213–227.

Nokleberg, W. J., Plafker, G., Lull, J. S., Wallace, W. K. and Winkler, G. W. (1989) Structural analysis of the southern Peninsular, southern Wrangellia, and northern Chugach terranes along the Trans-Alaska Crustal Transect (TACT), northern Chugach Mountains, Alaska. *Journal of geophysical Research* **94**, 4297–4320.

Nokleberg, W. J., Plafker, G. and Wilson, F. H. (1994) Geology of south-central Alaska. In *The Geology of Alaska, Decade of North American Geology*, **G-1**, eds G. Plafker and H. C. Berg. Geological Society America Press, Denver, 311–366.

Pavlis, T. L. and Crouse, G. W. (1989) Late Mesozoic strike-slip movement on the Border Ranges Fault system in the Eastern Chugach Mountains Southern Alaska. *Journal of geophysical Research* **94**, 4321–4332.

Pavlis, T. and Sisson, V. B. (1995) Structural history of the Chugach metamorphic complex in the Tana River region, eastern Alaska: A record of Eocene ridge subduction. *Bulletin of geological Society America* **107**, 1333–1355.

Pickthorn, W. J. 1982. Stable isotope and fluid inclusion study of the Port Valdez district, southern Alaska. Unpublished M.S. Thesis, University of California.

Plafker, G. (1983) The Yakutat block: an actively accreting tectono-stratigraphic terrane in southern Alaska. *Geological Society America, Abstracts with Programs* **15**, 406.

Plafker, G. and Berg, H. C. 1994. Overview of the geology and tectonic evolution of Alaska. In *The Geology of Alaska, Decade of North American Geology*, **G-1**, eds G. Plafker and H. C. Berg. Geological Society America Press, Denver, 389–449.

Plafker, G., Moore, J. C. and Winkler, G. R. 1994. Geology of the Southern Alaska Margin. In *The Geology of Alaska, Decade of North American Geology*, **G-1**, eds G. Plafker and H. C. Berg. Geological Society America Press, Denver, 989–1022.

Plafker, G., Nokleberg, W. J. and Lull, J. S. (1989) Bedrock geology and tectonic evolution of the Wrangellia, Peninsular, and Chugach terranes along the Trans-Alaska crustal transect in the northern Chugach Mountains and southern Copper River basin Alaska. *Journal of geophysical Research* **94**, 4255–4295.

Platt, J. P. (1986) Dynamics of orogenic wedges and the uplift of high-pressure metamorphic rocks. *Bulletin geological Society America* **97**, 1037–1053.

Pollard, D. D., Saltzer S. D. and Rubin, A. M. (1993) Stress inversion methods: are they based on faulty assumptions? *Journal of Structural Geology* **15**, 1045–1054.

Reches, Z. (1978) Analysis of faulting in three-dimensional strain field. *Tectonophysics* **47**, 109–129.

Reches, Z. (1983) Faulting of rocks in three-dimensional strain fields II. Theoretical analysis. *Tectonophysics* **95**, 133–156.

Reches, Z. and Dieterich, J. H. (1983) Faulting of rocks in three-dimensional strain fields I. Failure of rocks in polyaxial, servo-control experiments. *Tectonophysics* **95**, 111–132.

Roeske, S. M., Pavlis, T. L., Snee, L. W. and Sisson, V. B. (1991) $^{40}Ar/^{39}Ar$ isotopic ages from the combined Wrangellia–Alexander Terrane along the Border Ranges Fault System in the eastern Chugach Mountains and Glacier Bay, Alaska. In *Geologic Studies in Alaska by the U.S. Geological Survey, 1990*, eds D.C. Bradley and A. Ford. *Bulletin of U.S. geological Survey* **1999**, 180–195.

Roeske, S. M., Snee, L. W. and Bunds, M. P. (1993) $^{40}Ar/^{39}Ar$ dates from the Border Ranges Fault System, a hydrothermally altered brittle–ductile transition strike-slip shear zone, southern Alaska. *Geological Society America, Abstracts with Programs* **25**, 419.

Sample, J. C. and Moore, J. C. (1987) Structural style and kinematics of an underplated slate belt, Kodiak and adjacent islands, Alaska. *Bulletin geological Society America* **99**, 7–20.

Silberman, M. L., Mitchell, P. A. and O'Neil, J. R. (1981) Isotopic data bearing on the origin and age of the epithermal lode gold deposits in the Hope-Sunrise mining district, northern Kenai Peninsula, Alaska. *U.S. geological Survey Circular* **823-B**, 81–B84.

Sisson, V. B., Hollister, L. S. and Onstott, T. C. (1989) Petrologic and age constraints on the origin of a low pressure/high temperature metamorphic complex, southern Alaska. *Journal of geophysical Research* **94**, 4392–4410.

Sisson, V. B. and Pavlis, T. (1993) Geologic consequences of plate reorganization: An example from the Eocene southern Alaska fore-arc. *Geology* **21**, 913–916.

Stock, J. and Molnar, P. (1988) Uncertainties and implications of the late Cretaceous and Tertiary positions of North America relative to the Farallon, Kula, and Pacific plates. *Tectonics* **7**, 1339–1384.

Stuwe, K. (1986) Structural evolution of the Port Wells gold mining district, Prince William Sound, south central Alaska: Implications for the origin of the gold lodes. *Mineral Deposits* **21**, 288–295.

Twiss, R. J. and Gefell, M. J. (1990) Curved slickenfibers: A new brittle shear sense indicator with an application to a sheared serpentinite. *Journal of Structural Geology* **12**, 471–481.

Twiss, R. J., Protzman, G. M. and Hurst, S. D. (1991) Theory of slickenline patterns based on the velocity gradient tensor and micro-rotation. *Tectonophysics* **186**, 215–239.

Wilkerson, M. S. and Marshak, S. (1991) Factors controlling slip lineation orientation on thrust-fault planes. *Tectonophysics* **196**, 203–208.

Winkler, G. R. 1992. Geologic map and summary geochronology of the Anchorage $1° \times 3°$ Quadrangle, southern Alaska. *U.S. geological Survey, Miscellaneous Investigations Series* Map I-2283, scale 1:250,000.

Wojtal, S. 1989. Day Seven — Valley and Ridge Province in southwest Virginia and northeast Tennessee. *International Geological Congress Guidebook* **T57**, 57–67.

Wojtal, S. F. (1996) Changes in fault displacement populations correlated to linkage between faults. *Journal of Structural Geology* **18**, 265–279.

Yin, Z. M. and Ranalli, G. (1992) Critical stress difference, fault orientation and slip direction in anisotropic rocks under non-Andersonian stress systems. *Journal of Structural Geology* **14**, 237–244.